Biochimica et Biophysica Acta 1842 (2014) 1154–1166

Contents lists available at ScienceDirect

Biochimica et Biophysica Acta

journal homepage: www.elsevier.com/locate/bbadis

Insulin therapy modulates mitochondrial dynamics and biogenesis, autophagy and tau protein phosphorylation in the brain of type 1 diabetic rats

R.X. Santos [a,b], S.C. Correia [b,c], M.G. Alves [d], P.F. Oliveira [d], S. Cardoso [a,b], C. Carvalho [a,b], A.I. Duarte [b,c], M.S. Santos [a,b], P.I. Moreira [b,e,*]

[a] Department of Life Sciences, Faculty of Sciences and Technology, University of Coimbra, Portugal
[b] CNC — Center for Neuroscience and Cell Biology, University of Coimbra, Coimbra, Portugal
[c] Institute for Interdisciplinary Research, University of Coimbra, Coimbra, Portugal
[d] CICS-UBI, Health Sciences Research Centre, University of Beira Interior, Covilhã, Portugal
[e] Laboratory of Physiology, Faculty of Medicine, University of Coimbra, Coimbra, Portugal

ARTICLE INFO

Article history:
Received 7 November 2013
Received in revised form 8 April 2014
Accepted 10 April 2014
Available online 18 April 2014

Keywords:
Autophagy
Cerebral cortex
Insulin treatment
Tau protein phosphorylation
Type 1 diabetes
Mitochondrial fission, fusion and biogenesis

ABSTRACT

The main purpose of this study was to examine whether streptozotocin (STZ)-induced type 1 diabetes (T1D) and insulin (INS) treatment affect mitochondrial function, fission/fusion and biogenesis, autophagy and tau protein phosphorylation in cerebral cortex from diabetic rats treated or not with INS. No significant alterations were observed in mitochondrial function as well as pyruvate levels, despite the significant increase in glucose levels observed in INS-treated diabetic rats. A significant increase in DRP1 protein phosphorylated at Ser616 residue was observed in the brain cortex of STZ rats. Also an increase in NRF2 protein levels and in the number of copies of mtDNA were observed in STZ diabetic rats, these alterations being normalized by INS. A slight decrease in LC3-II levels was observed in INS-treated rats when compared to STZ diabetic animals. An increase in tau protein phosphorylation at Ser396 residue was observed in STZ diabetic rats while INS treatment partially reversed that effect. Accordingly, a modest reduction in the activation of GSK3β and a significant increase in the activity of phosphatase 2A were found in INS-treated rats when compared to STZ diabetic animals. No significant alterations were observed in caspases 9 and 3 activity and synaptophysin and PSD95 levels. Altogether our results show that mitochondrial alterations induced by T1D seem to involve compensation mechanisms since no significant changes in mitochondrial function and synaptic integrity were observed in diabetic animals. In addition, INS treatment is able to normalize the alterations induced by T1D supporting the importance of INS signaling in the brain.

1. Introduction

Type 1 diabetes (T1D) is a metabolic disease that originates from the autoimmune destruction of β-cells due to lymphocytic infiltration of pancreatic islets, resulting in the permanent dependency of patients on exogenous insulin (INS) to survive [1].

Cognitive deficits, such as impaired learning, memory, problem solving, and mental flexibility have been recognized as being more common in T1D subjects than in the general population [2,3]. It has also been demonstrated that T1D exacerbates tau protein hyperphosphorylation and amyloid beta (Aβ) formation contributing to the deposition of neurofibrillary tangles and Aβ plaques, the two major pathological hallmarks of Alzheimer's disease (AD), in the amyloid precursor protein (APP) transgenic mice [4].

INS has been proven to exert a role in synaptic plasticity and memory consolidation through the modulation of the activity of excitatory and inhibitory receptors such as those for glutamate and GABA, and by triggering signal transduction cascades leading to the alteration of gene expression [5,6]. Furthermore, INS and insulin-like growth factors (IGFs) have been shown to protect neurons against Aβ toxicity [7,8]. Likewise, insulin reduced tau protein phosphorylation and promoted its binding to microtubules, the effects of INS being mediated through the inhibition of glycogen synthase kinase-3β (GSK-3β) via the phosphoinositide 3-kinase (PI3-K)/Akt signaling pathway [9].

Mitochondria account for more than 90% of the cellular energy production [10]. This bioenergetic production assumes its maximum importance in the brain since neurons have a high energy demand and a limited glycolytic capacity, making them highly dependent on aerobic oxidative phosphorylation [11].

* Corresponding author at: Laboratory of Physiology, Faculty of Medicine, University of Coimbra & Center for Neuroscience and Cell Biology, University of Coimbra, 3004-517 Coimbra, Portugal.
E-mail addresses: venta@ci.uc.pt, pimoreira@fmed.uc.pt (P.I. Moreira).

http://dx.doi.org/10.1016/j.bbadis.2014.04.011
0925-4439/

Mitochondrial network is maintained through the fine balance between mitochondrial fission and fusion. Mitochondrial fission is governed by dynamin-like protein 1 (DRP1), a large cytosolic GTPase that is recruited to the mitochondrial membrane upon a fission-like stimuli, and by Fis1, a small mitochondrial molecule located in the outer membrane [12]. In turn, mitochondrial fusion is directed by three large GTPases, Mitofusin 1 (Mfn1) and Mitofusin 2 (Mfn2), both located in the mitochondrial outer membrane, and optic atrophy 1 (OPA1) protein, located in the inner mitochondrial membrane [12].

Mitochondrial biogenesis results from an intricate crosstalk between both nuclear and mitochondrial genomes. The molecular machinery underlying mitochondrial biogenesis is constituted by the nuclear respiratory factor 1 (NRF 1) and nuclear respiratory factor 2 (NRF 2), which control the nuclear genes that encode mitochondrial proteins, and mitochondrial transcription factor A (TFAM) that drives transcription and replication of mitochondrial (mt) DNA [13,14]. The expression of NRF1, NRF2, and TFAM is regulated by the peroxisome proliferator activator receptor gamma-coactivator 1α (PGC-1α) [15].

Autophagy is an evolutionarily conserved housekeeping process that enables cells to get nutrients through the digestion of their own components and, at the same time, degrades misfolded proteins and aggregates, damaged organelles and invading microorganisms [16]. Autophagy is a tightly regulated process in a multistep manner. To the level of vesicle nucleation/initiation two main proteins are involved: the mammalian target of rapamycin (mTOR), which is an autophagic repressor; and Beclin 1, which is an autophagic inducer [17]. Regarding membrane elongation, cytosolic LC3-I is transformed to a membrane-bound form, LC3-II [17]. In the autophagic degradation of ubiquitinated protein aggregates in mammalian cells, LC3 interacts with p62, which is a ubiquitin-binding protein therefore being considered an autophagic substrate [17].

The main aim of this study was the evaluation of the effects of streptozotocin (STZ)-induced T1D and INS treatment on brain cortical mitochondria, autophagy and tau protein phosphorylation. We evaluated several mitochondrial parameters: respiration [respiratory control ratio (RCR), and ADP/O index], phosphorylation system [transmembrane potential (ΔΨm), ADP-induced depolarization, repolarization lag phase], fission/fusion protein levels (DRP1, Fis 1 and OPA1, MFN1, MFN2, respectively), and biogenesis (NRF1, NRF2, TFAM and the number of copies of mtDNA). Autophagy (mTOR, Beclin1, LC3 and p62 protein levels), the activity of several kinases and phosphatase 2A that modulate tau protein phosphorylation, activity of caspases 3 and 9 and protein levels of synaptophysin and PSD95 were also evaluated.

2. Material and methods

2.1. Reagents

STZ was obtained from Sigma Aldrich (St. Louis, MO, USA). INS (Humulin NPH) was obtained from Eli Lilly and Company (USA). All the chemicals used were of the highest grade of purity commercially available.

2.2. Animal housing and treatment

Seventeen male Wistar rats (2-month-old) purchased from Charles River were housed in our Animal Facility (Laboratory Research Center, Faculty of Medicine, University of Coimbra) and maintained under controlled light (12 h day/night cycle) and humidity with ad libitum access to water and powdered rodent chow (except in the fasting period). Rats were deprived of food overnight and randomly divided into two groups. One group of eleven animals received an intraperitoneal (i.p.) injection of STZ (50 mg/kg body weight) freshly dissolved in 100 mM citrate, pH 4.5. The volume administered was always 0.5 ml/200 g body weight. The control group (six animals) received an i.p. injection with an equal volume of citrate (vehicle solution). In the following 24 h, animals were provided with free access to glycosylated serum in order to avoid hypoglycemia resulting from the massive destruction of β-cells and consequent release of intracellular insulin associated with STZ treatment [18]. Three days after STZ administration, the tail vein blood glucose levels were measured in all animals and those presenting levels above 250 mg/dl were considered diabetic. Two months after the induction of diabetes with STZ, diabetic rats were randomly divided into two groups and one group of six animals was subjected to daily subcutaneous (s.c.) injections of INS, in order to lower the systemic levels of glucose (dose adjusted to blood glucose levels as follows: if blood glucose levels were ≤200 mg/dL, 2 U INS were administered to rats; if blood glucose levels were >200 mg/dL an extra 2 U INS per each 100 mg/dL blood glucose were given to rats), during one month. Three months after the induction of diabetes, the rats were sacrificed by cervical displacement and decapitation. Animal handling and sacrifice followed the procedures approved by the Federation of European Laboratory Animal Science Associations (FELASA).

2.3. Measurement of blood glucose and hemoglobin A1C levels

Blood glucose was determined immediately after sacrifice by a glucose oxidase reaction, using a glucometer (Glucometer-Elite, Bayer). Hemoglobin A1C (HbA1c) levels were determined using Systems SYNCHRON CX 4 (Beckman). This system utilizes two cartridges, Hb and A1c to determine A1c concentration as a percentage of the total Hb. The hemoglobin is measured by a colorimetric method and the A1c concentration by a turbidimetric immunoinhibition method.

2.4. Measurement of brain INS, glucose and pyruvate levels

Brain cortical tissues were homogenized in radioimmunoprecipitation assay (RIPA) buffer containing 0.1 M phenylmethylsulfonyl fluoride (PMSF), 0.2 M dithiothreitol (DTT), and protease and phosphatase inhibitors (commercial protease and phosphatase inhibitor cocktails from Roche Applied Science). The crude homogenate was incubated on ice for 15 min, frozen and defrozen 3 times to favor disruption, and centrifuged at 14000 rpm (Eppendorf centrifuge 5415C) for 10 min, at 4 °C, and the resulting supernatant was collected and stored at −80 °C.

INS quantification was performed using an ELISA kit (BertinPharma, France) according to the manufacturers' instructions. The principle of the kit is based on the competition between unlabeled rat insulin and acetylcholinesterase (AChE) linked to rat insulin (tracer) for limited specific Guinea-Pig anti-rat insulin antiserum sites.

Glucose quantification was performed using a PicoProbe™ glucose fluorometric assay kit (BioVision, USA) according to manufacturers' instructions. The principle of the kit is based on the enzymatic oxidation of D-glucose to form a product which reacts with a colorless probe to generate fluorescence. The fluorescence generated is directly proportional to the amount of glucose present in the sample.

Pyruvate quantification was performed using a pyruvate colorimetric assay kit (BioVision, USA) according to the manufacturers' instructions. The principle of the kit is based on the enzymatic oxidation of pyruvate by pyruvate oxidase to generate color upon reaction with a pyruvate probe. The color intensity is proportional to pyruvate content; therefore the pyruvate concentration can be accurately measured.

2.5. Preparation of mitochondrial fractions

Brain cortical mitochondria were isolated from rats by the method of Moreira et al. [19], using 0.02% digitonin to allow the release of mitochondria from the synaptosomal fraction. Briefly, after animal decapitation, the cortex was immediately separated and homogenized at 4 °C in 10 ml of isolation medium (225 mM mannitol, 75 mM sucrose, 5 mM HEPES, 1 mM EGTA, 1 mg/ml BSA, pH 7.4) containing 5 mg of the bacterial protease (Sigma). Single brain homogenates were brought to 30 ml and then centrifuged at 2500 rpm (Sorvall Evolution RC Superspeed

Refrigerated Centrifuge) for 5 min. The resulting supernatant was then centrifuged at 10,000 rpm for 10 min. The pellet, including the fluffy synaptosomal layer, was resuspended in 10 ml of the isolation medium containing 0.02% digitonin and centrifuged at 10,000 rpm for 10 min. The brown mitochondrial pellet without the synaptosomal layer was resuspended again in 10 ml of medium and centrifuged at 10,000 rpm for 5 min. The pellet was resuspended in 10 ml of washing medium (225 mM mannitol, 75 mM sucrose, 5 mM HEPES, pH 7.4) and centrifuged at 10,000 rpm for 5 min. The final mitochondrial pellet was resuspended in the washing medium and the protein amount was determined by the biuret method calibrated with bovine serum albumin (BSA) [20].

2.6. Measurements of mitochondrial respiration

Oxygen consumption of mitochondria was registered polarographically with a Clark oxygen electrode [21] connected to a suitable recorder in a thermostated water-jacketed closed chamber with magnetic stirring. The reactions were carried out at 30 °C in 1 ml of standard respiratory medium (100 mM sucrose, 100 mM KCl, 2 mM KH_2PO_4, 5 mM Hepes and 10 μM EGTA; pH 7.4) with 0.5 mg of protein. State 3 of respiration (consumption of oxygen in the presence of substrate and ADP) was initiated with the addition of exogenous ADP (50 nmol/mg protein). States 3 and 4 (consumption of oxygen after ADP phosphorylation) of respiration, respiratory control ratio (RCR = state 3/state 4), and ADP/O index (a marker of the mitochondrial ability to couple oxygen consumption to ADP phosphorylation during state 3 of respiration) were determined according to [22]. FCCP-stimulated respiration was also measured as a state of uncoupled respiration, i.e. respiratory chain maximal activity [23]. Oligomycin-inhibited respiration was also measured representing oxygen consumption with inhibited ATP synthase, which is due to proton leak [23].

2.7. Measurements of $\Delta\Psi_m$

The transmembrane potential ($\Delta\Psi_m$) was monitored by evaluating the transmembrane distribution of the lipophilic cation TPP^+ (tetraphenylphosphonium) with a TPP^+-selective electrode prepared according to Kamo et al. [24] using an Ag/AgCl-saturated electrode (Tacussel, model MI 402) as reference. TPP^+ uptake has been measured from the decreased TPP^+ concentration in the medium sensed by the electrode. The potential difference between the selective electrode and the reference electrode was measured with an electrometer and recorded continuously in a Linear 1200 recorder. The voltage response of the TPP^+ electrode to log[TPP^+] was linear with a slope of 59 ± 1, which is in a good agreement with the Nernst equation. Reactions were carried out in a chamber with magnetic stirring in 1 ml of the standard medium (100 mM sucrose, 100 mM KCl, 2 mM KH_2PO_4, 5 mM Hepes and 10 μM EGTA; pH 7.4) containing 3 μM TPP^+. This TPP^+ concentration was chosen in order to achieve high sensitivity in measurements and to avoid possible toxic effects on mitochondria [25]. The $\Delta\Psi_m$ was estimated by the equation: $\Delta\Psi_m\,(mV) = 59\log(v/V) - 59\log(10^{\Delta E/59} - 1)$, as indicated by Kamoet al. [24] and Muratsugu et al. [26]. v, V, and ΔE stand for mitochondrial volume, volume of the incubation medium and deflection of the electrode potential from the baseline, respectively. This equation was derived assuming that TPP^+ distribution between the mitochondria and the medium follows the Nernst equation, and that the law of mass conservation is applicable. A matrix volume of 1.1 μl/mg protein was assumed. No correction was made for the "passive" binding contribution of TPP^+ to the mitochondrial membranes, because the purpose of the experiments was to show relative changes in potentials rather than absolute values. As a consequence, we can anticipate a slight overestimation on $\Delta\Psi_m$ values. However, the overestimation is only significant at $\Delta\Psi_m$ values below 90 mV, therefore, far from our measurements. Mitochondria (0.5 mg/ml) were energized with 5 mM succinate (substrate of complex II) in the presence of 2 μM rotenone in order to activate the mitochondrial electron transport chain. After a steady-state distribution of TPP^+ had been reached (ca. 1 min of recording), $\Delta\Psi_m$ fluctuations were recorded.

2.8. Protein extraction for Western blot analysis

Brain cortical tissues were homogenized in RIPA buffer containing 0.1 M PMSF, 0.2 M DTT, and protease and phosphatase inhibitors (commercial protease and phosphatase inhibitor cocktails from Roche Applied Science). The crude homogenate was incubated on ice for 15 min, frozen and defrozen 3 times to favor disruption, and centrifuged at 14,000 rpm (Eppendorf centrifuge 5415C) for 10 min, at 4 °C, and the resulting supernatant was collected and stored at −80 °C. The amount of protein content in the samples was analyzed by the bicinchoninic acid (BCA) protein assay using the BCA kit (Pierce Thermo Fisher Scientific, Rockford, IL).

2.9. Western blot analysis

Samples (50–75 μg per lane) were resolved by electrophoresis in 8–15% sodium dodecyl sulfate (SDS)–polyacrylamide gels and transferred to polyvinylidenedifluoride (PVDF) membranes. Non-specific binding was blocked by gently agitating the membranes in 5% non-fat milk or 5% BSA for phosphoproteins and 0.05% Tween in Tris-buffered saline (TBS) for 1 h at room temperature. The blots were subsequently incubated with specific primary antibodies, overnight at 4 °C, with gentle agitation. The blots were washed 3 times (15 min), with Tris buffer containing 0.05% Tween (TBS-T) and then incubated with secondary antibodies for 1 h at room temperature with gentle agitation. After 3 washes with TBS-T specific bands of immunoreactive proteins were visualized after membrane incubation with enhanced chemifluorescence (ECF) for 5 min in a VersaDoc Imaging System (Bio-Rad), and the density of protein bands was calculated using the Quantity One Program (Bio-Rad).

In some cases, the same membrane was used to detect other proteins with very different molecular weights. In these situations, the membranes were gently washed with 40% methanol (30 min) and 3 times (15 min) with TBS-T and then incubated with the primary antibody. The following steps are identical to those described above.

Total and respective phosphorylated protein levels were examined in two distinct membranes. To preserve data accuracy the following procedures were adopted: 1) the same sample was used to analyze total and phosphorylated protein levels; 2) all samples had the same cycles of freezing and thawing (reduced to a minimum); 3) the two gels were prepared and ran at the same time; 4) after proteins have been transferred onto PVDF membranes and stained with specific antibodies, each band of interest were normalized with respect to the loading control (actin); and 5) the ratio between phosphorylated and total protein levels was obtained by the formula (phosphorylated protein/actin membrane 1)/(total protein/actin membrane 2).

The primary antibodies used were: anti-P^{ser396} Tau (1:1000; Santa Cruz Biotechnology); anti-P^{thr181} Tau (1:250; Santa Cruz Biotechnology); anti-Tau (BT2) (1:1000; Thermo Scientific); anti-P^{ser9} GSK3β (1:1000; Cell Signaling); anti-P^{tyr216} GSK3β (1:500; Santa Cruz Biotechnology); anti-GSK3β (1:500; Santa Cruz Biotechnology); anti-$P^{thr183/tyr185}$ JNK (1:2000; Cell Signaling); anti-JNK (1:1000; Cell Signaling); anti-$P^{thr202/tyr204}$ ERK (1:1000; Cell Signaling); anti-ERK (1:1000; Cell Signaling); anti-$P^{thr180/tyr182}$ p38 MAPK (1:1000; Cell Signaling); anti-p38 MAPK (1:1000; Cell Signaling); anti-Synaptophysin (1:20,000; Sigma Aldrich);anti-PSD95 (1:1000; Cell Signaling); anti-Mfn1 (1:1000; Santa Cruz Biotechnology); anti-Mfn2 (1:1000; Santa Cruz Biotechnology); anti-OPA1 (1:1000; BD Biosciences); anti-Fis1 (1:750; Imgenex); anti-DRP1 (1:1000; BD Biosciences); anti-P^{ser616} DRP1 (1:1000; Cell Signaling); anti-mTOR (1:1000; Cell Signaling); anti-$P^{ser2448}$ mTOR (1:1000; Cell Signaling); anti-Beclin 1 (1:1000; BD Biosciences); anti-LC3 (1:1000; Sigma); anti-p62

Table 1
Oligonucleotides and cycling conditions for qPCR amplification of ND1 and β-2-microglobulin.

Gene	Sequence (5′–3′)	AT (°C)	Amplificon size (bp)	C
ND1	Sense: GAG CCC TAC GAG CCG TTG CC Antisense: GCG AATG GTC CTG CGG CGT A	58	271	30
β2MG	Sense: GCG TGG GAG GAG CAT CAG GG Antisense: CTC ATC ACC ACC CCG GGG ACT	58	264	30

Abbreviations: AT — annealing temperature; C — Number of cycles of amplification

(1:1000; Sigma); anti-NRF1 (1:500; Santa Cruz Biotechnology); anti-NRF2 (1:500; Abcam); anti-TFAM (1:1000; Santa Cruz Biotechnology); anti-MTCOI (1:1000; Abcam); anti-α-Tubulin (1:1000; Cell Signaling); and anti-β actin (1:5000; Sigma). The secondary antibodies used were: anti-mouse IgG alkaline phosphatase conjugate (1:10,000; Amersham Pharmacia Biotech); anti-rabbit IgG alkaline phosphatase conjugate (1:10,000; Amersham Pharmacia Biotech); anti-goat IgG alkaline phosphatase conjugate (1:2500; Santa Cruz Biotechnology).

2.10. Measurement of phosphatase 2A activity

Phosphatase 2A (PP2A) activity was measured using a PP2A DuoSet IC kit (R&D Systems) according to the manufacturer's instructions. Briefly, a portion of brain tissue was homogenized in ice cold lysis buffer (Cell Signaling) and 75 μg of protein were loaded onto 96-well plates coated with a capture antibody specific for PP2A (R&D Systems) for immunocapture at 4 °C for 3 h. After washing twice, synthetic phosphopeptide substrates (200 μM) were added for the dephosphorylation reaction catalyzed by PP2A. The level of free phosphate was determined by a sensitive dye-binding assay using malachite green and molybdic acid according to the manufacturer's instructions followed by measurement of the absorbance at 620 nm.

2.11. Measurement of caspases 3 and 9 activation

Caspases 3 and 9 activation was measured using a colorimetric method. Brain cortical tissues were homogenized in cold RIPA buffer and frozen and defrozen 3 times. The lysates were centrifuged for 10 min at 14,000 rpm (5417R, Eppendorf) at 4 °C. The resulting supernatant was stored at −80 °C. Protein concentrations were measured by using the BCA protein assay kit (Pierce, Rockford, IL).

Samples (50 μg of protein) were incubated at 37 °C for 2 h in 25 mM Hepes, pH 7.5 containing 0.1% 3-[(3-cholamido-propyl) dimethylammonio]-1-propanesulfonate (CHAPS), 10% sucrose, 2 mM DTT, and 40 μM Ac-DEVD-pNA for caspase 3 or 40 μM Ac-LEHD-pNA for caspase 9. Caspase 3- and caspase 9-like activity was determined by measuring substrate cleavage at 405 nm in a microplate reader (SpectraMax Plus 384, Molecular Devices).

2.12. Determination of mtDNA copy number

Total DNA was extracted from brain cortical tissues using the TRIzol Reagent (Sigma-Aldrich) according to the manufacturer's instructions. Real-time qPCR analysis was performed to determine the mtDNA copy number as described by Fuke and collaborators [27], with slight modifications. Relative quantification of mtDNA levels was determined by the ratio of the mitochondrial ND1 (mt-Nd1) gene to the single-copy, nuclear-encoded beta-2-microglobulin (β2MG) gene. Reactions were carried out in an iQ5 system (Bio-Rad), and the efficiency of the reactions was determined for the selected primers using serial dilutions of DNA samples. Primer concentration and annealing temperature were optimized, and the specificity of the amplicons was determined by melting curve analysis. The reaction mixture consisted of Maxima SYBR Green qPCR Master Mix (Fermentas), sense and antisense primers (see Table 1 for details), and 20 ng of DNA. Each reaction was run in triplicate to calculate relative mtDNA copy number. Control values of all samples were within the linear range. Control value differences were used to quantify mtDNA copy number relative to the beta-2-microglobulin gene with the following equation: Relative copy number $= 2^{\Delta Ct}$, where ΔCt is $Ct_{\beta 2MG} - Ct_{ND1}$.

2.13. Statistical analysis

Data regarding the characterization of the experimental animal groups and mitochondrial function parameters are presented as mean ± SEM of the indicated number of animals and differences between groups were analyzed using one-way ANOVA followed by Tukey's post-hoc test. All other data are expressed as median ± interquartile range of the indicated number of animals and statistical significance was determined using the non-parametric test of Kruskal–Wallis followed by the post-hoc Dunn's multiple comparison test.

3. Results

3.1. Characterization of the experimental animal models

STZ animals present a significant reduction in their body weight, and a significant increase in glycemia and glycated hemoglobin (HbA1c), when compared to Wistar (W) control rats (Table 2), confirming their diabetic state. Compared to untreated STZ diabetic rats, diabetic rats treated with INS present a statistically significant increase in body weight and a significant reduction in glycemia and HbA1c levels, which demonstrates the effectiveness of INS treatment in the amelioration of the diabetic phenotype. Additionally, a decrease in INS brain cortical levels is observed in STZ animals, an effect that is partially reversed by INS treatment (Fig. 1A). INS-treated rats show an increase in the levels of brain glucose (Fig. 1B), although no statistically significant alterations are observed in pyruvate levels (Fig. 1C).

3.2. Neither T1D nor INS treatment affect mitochondrial function

RCR is a measure of the coupling between substrate oxidation and phosphorylation and is a good indicator of mitochondrial integrity. ADP/O index shows the efficiency of the mitochondrial phosphorylative system [23]. Both mitochondrial indexes present no significant differences between the experimental groups (Table 3). Also FCCP and oligomycin respiratory states show no significant differences between the experimental groups (Table 3).

Mitochondrial membrane potential ($\Delta\Psi_m$) is generated through the respiratory chain pumping of protons from the mitochondrial matrix to

Table 2
Characterization of the experimental animal models.

	Body weight (g)	Brain weight (g)	Glycemia (mg/dL)	HbAlc (%)
Wistar	457.2 ± 24.70	2.29 ± 0.07	92.60 ± 2.27	3.53 ± 0.03
STZ	261.2 ± 10.72***	2.16 ± 0.10	502.5 ± 29.90***	9.66 ± 0.53***
INS	332.2 ± 7.27*** #	2.05 ± 0.10	347.2 ± 36.61*** ##	6.15 ± 0.27*** ###

Data are the mean ± SEM of 6 animals from each condition studied. Statistical significance: ***$p < 0.001$ when compared to the respective Wistar control rats; #$p < 0.05$, ##$p < 0.001$ and ###$p < 0.001$ when compared to the respective STZ diabetic rats.

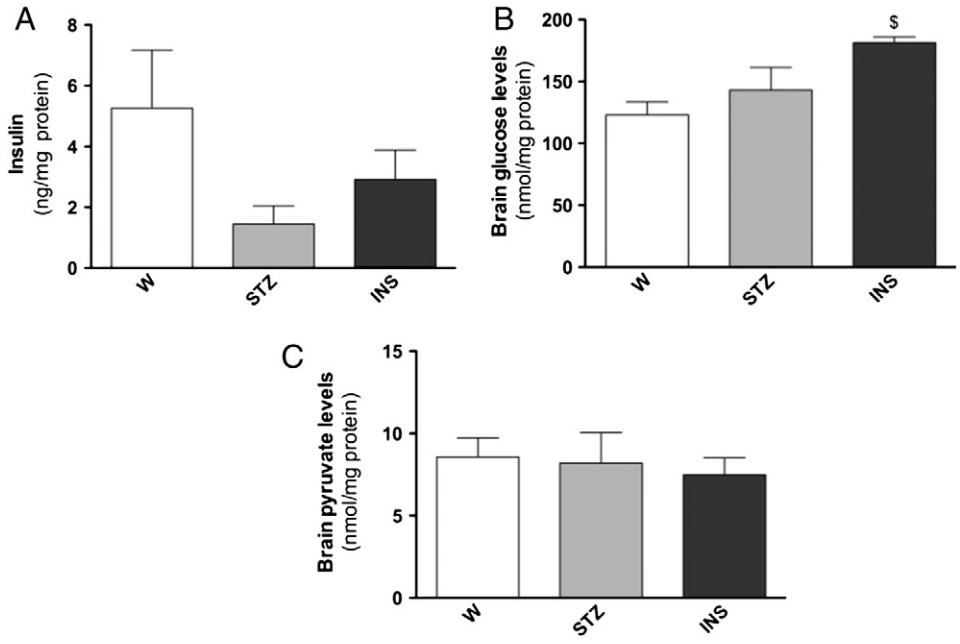

Fig. 1. Effects of T1D (STZ-induced diabetes) and insulin (INS) treatment in brain cortical insulin (A), glucose (B) and pyruvate (C) levels. Data are the mean ± SEM of 5–6 animals from each condition studied. Statistical significance: $^{\$}p < 0.05$ when compared to the respective Wistar (W) control animals.

the intermembrane space. The proton gradient originates an electrochemical potential (Δp) resulting in a pH (ΔpH) and a voltage gradient ($\Delta\Psi_m$) across the inner membrane. No statistically significant differences are observed in $\Delta\Psi_m$ and ADP-induced depolarization between the three experimental groups of animals (Table 3). Lag phase is the time necessary for mitochondria to phosphorylate the added ADP into ATP. Again, no statistically significant differences are observed between the experimental groups (Table 3).

3.3. INS reverses mitochondrial fission promoted by T1D

Regarding mitochondrial fusion, no significant alterations are observed in Mfn1 (Fig. 2A), Mfn2 (Fig. 2B) and OPA1 (Fig. 2C) protein levels. The mitochondrial fission-related protein Fis1 is statistically unaltered between the experimental groups (Fig. 3A) however, the active form of the fission protein DRP1 (P^{Ser616}-DRP1) is significantly increased in diabetic animals when compared to control animals, this effect being reversed by INS treatment (Fig. 3B).

Table 3
Effects of T1D (STZ-induced diabetes) and insulin (INS) treatment in brain cortical mitochondrial respiration and oxidative phosphorylation system.

		Wistar	STZ	INS
Respiratory parameters	RCR	4.65 ± 0.314	4.50 ± 0.157	4.51 ± 0.129
	ADP/O (nmol ADP/nAtgO/min/mg)	2.10 ± 0.299	2.10 ± 0.280	2.23 ± 0.201
	FCCP-stimulated respiration (nAtgO/min/mg)	97.39 ± 6.080	106.4 ± 23.64	100.1 ± 15.31
	Oligomycin-inhibited respiration (nAtgO/min/mg)	25.09 ± 4.070	29.12 ± 5.656	24.18 ± 3.451
Membrane potential and oxidative phosphorylation	$\Delta\Psi_m$ (-mV)	185.4 ± 0.73	185.2 ± 2.73	184.8 ± 1.53
	ADP-induced depolarization (-mV)	19.79 ± 1.51	20.21 ± 2.99	17.34 ± 0.80
	Lag phase (min)	0.97 ± 0.083	0.92 ± 0.053	0.88 ± 0.071

Data are the mean ± SEM of 6 animals from each condition studied.

3.4. INS treatment reverses T1D-induced mitochondrial biogenesis alterations

Several transcription factors have been enrolled in the transcription of genes that are crucial to mitochondria. To ascertain the role of T1D in brain cortical mitochondrial biogenesis the protein levels of NRF1 (Fig. 4A), NRF2 (Fig. 4B) and TFAM (Fig. 4C) were evaluated. STZ-induced T1D induces a significant increase in the levels of NRF2 (Fig. 4B) and a slight increase in the levels of TFAM (Fig. 4C), these effects being reversed by INS treatment (Fig. 4A–C). Accordingly, a significant increase in the relative number of mtDNA copies is observed in STZ diabetic animals (Fig. 5). Again, INS treatment tends to normalize the increase in the number of mtDNA copies induced by STZ-induced T1D (Fig. 5).

3.5. INS therapy modulates autophagy

mTOR is a recognized repressor of the autophagic pathway. As shown, the active form of mTOR ($P^{Ser2448}$-mTOR) (Fig. 6A) is not significantly altered in the three experimental groups. The same occurs with the autophagic inducer Beclin1 (Fig. 6B) and the autophagic substrate p62 (Fig. 6D). However, the levels of LC3-II, a gold-standard marker of autophagic vesicle elongation, are tendentiously decreased by INS treatment (Fig. 6C).

3.6. INS partially reverses tau protein phosphorylation promoted by T1D by the increase in PP2A activity

To investigate whether T1D and INS treatment affect tau protein phosphorylation, we evaluated the levels of tau protein phosphorylated at residues Ser396 and Thr181. T1D increases the protein levels of P^{Ser396}-Tau and decreases the protein levels of P^{Thr181}-Tau, while INS partially reverses these effects (Fig. 7). The protein levels of some

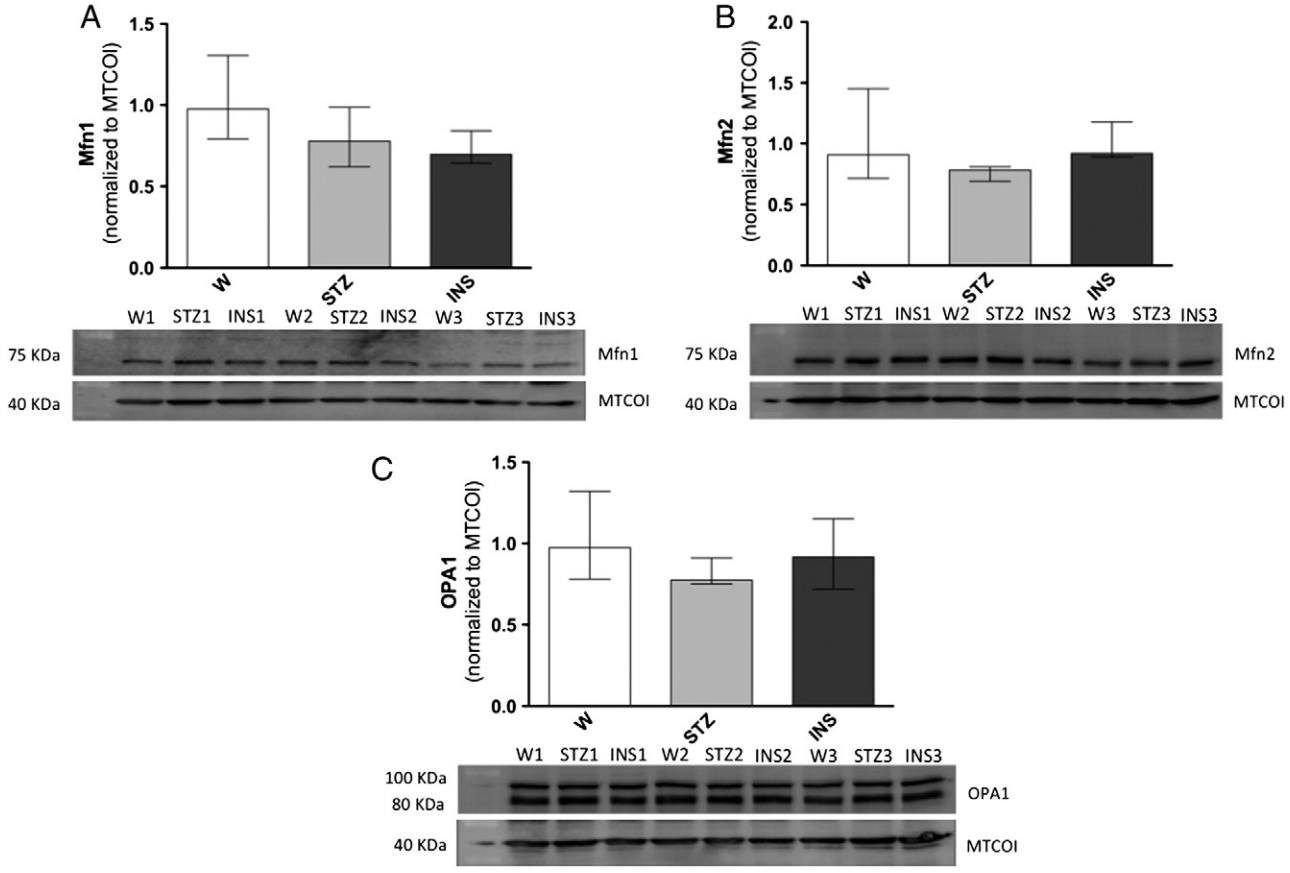

Fig. 2. Effects of T1D (STZ-induced diabetes) and insulin (INS) treatment in the levels of mitochondrial fusion-related proteins: Mfn1 (A), Mfn2 (B) and OPA1 (C). Data are the median ± interquartile range of 6 animals from each condition studied.

kinases involved in tau protein phosphorylation were also assessed. T1D does not significantly alter the levels of the active form of GSK3β (P^{Tyr216}-GSK3β) (Fig. 8A and B), however INS treatment tends to reduce the active form of this enzyme when compared to diabetic animals. A slight decrease in the levels of the inactive form of GSK3β (P^{Ser9}-GSK3β) is also observed in INS-treated rats (Fig. 8A and B). No significant alterations are observed in other kinases (JNK, ERK and p38 MAPK) known to modulate tau protein phosphorylation (Fig. 8A and B). Although not

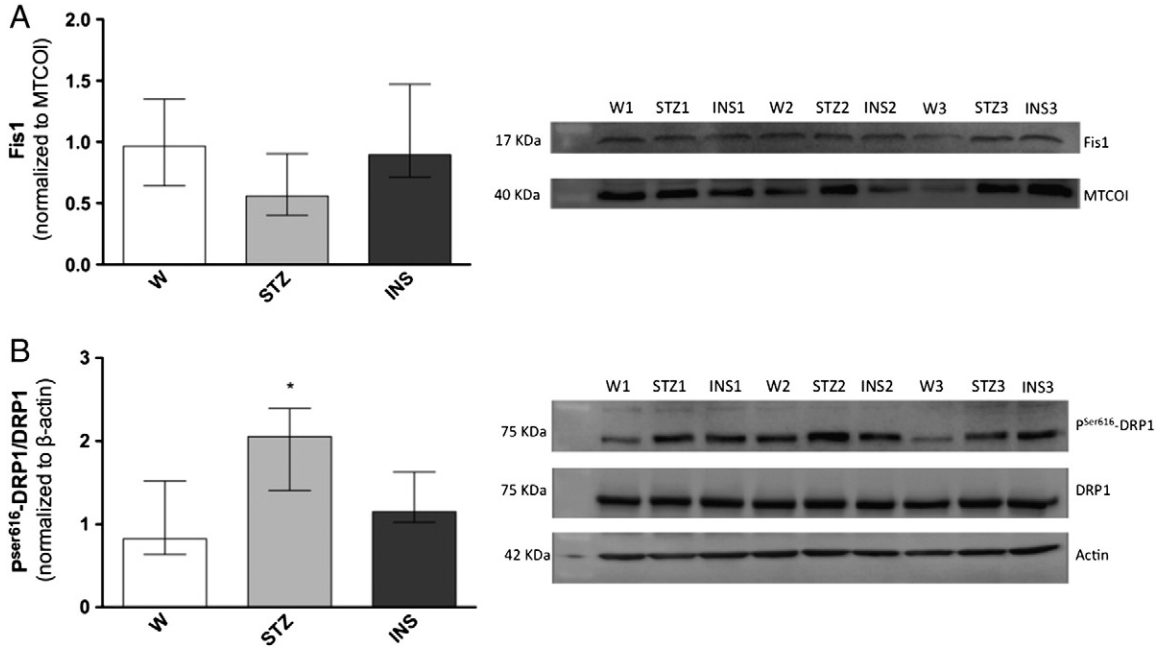

Fig. 3. Effects of T1D (STZ-induced diabetes) and insulin (INS) treatment in the levels of mitochondrial fission-related proteins: Fis1 (A) and P^{ser616}-DRP1/DRP1 (B). Data are the median ± interquartile range of 6 animals from each condition studied. Statistical significance: *$p < 0.05$ when compared to the respective Wistar (W) control animals.

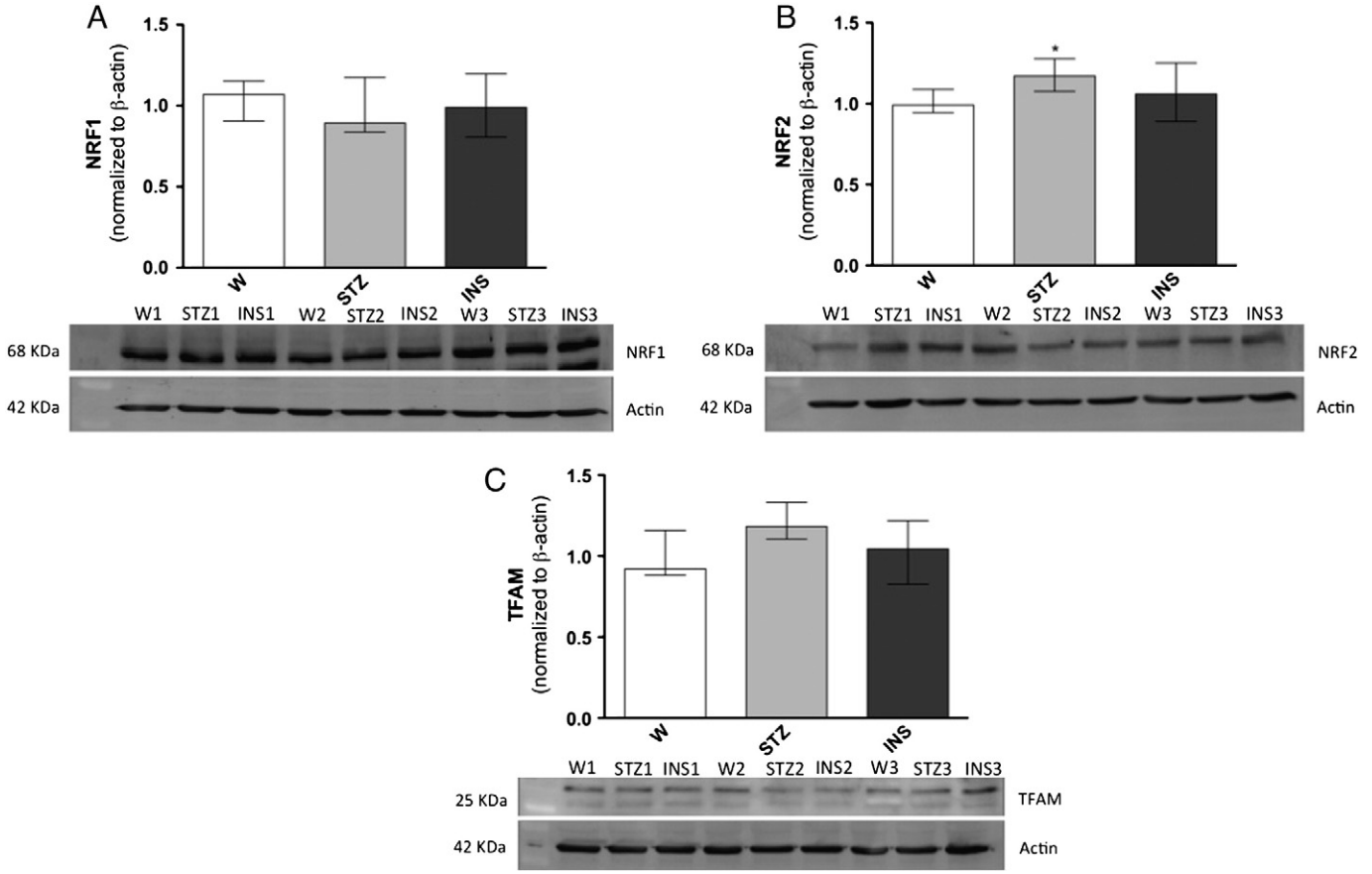

Fig. 4. Effects of T1D (STZ-induced diabetes) and insulin (INS) treatment in the levels of transcription factors related with mitochondrial biogenesis: NRF1 (A); NRF2 (B) and TFAM (C). Data are the median ± interquartile range of 6 animals from each condition studied. Statistical significance: *$p < 0.05$ when compared to the respective Wistar (W) control animals.

statistically significant, T1D decreases the activity of PP2A (Fig. 9) while INS treatment significantly increases the activity of this phosphatase when compared to diabetic animals (Fig. 9).

3.7. Neither T1D nor INS treatment alter brain cells survival and synaptic integrity

The initiator caspase 9 is responsible for the mitochondrial-dependent apoptotic cell death. Caspase 3 is an effector caspase involved in both extrinsic and intrinsic (i.e. mitochondrial pathway) apoptosis pathways. Both STZ-induced diabetes and INS treatment do not alter caspases 9- and 3-like activities (Fig. 10A and B, respectively), which is indicative of no effects on apoptotic cell death. Likewise, synaptophysin and PSD95 levels are not altered in the three experimental groups (Fig. 11A and B, respectively), which suggests that there is no significant loss of synaptic integrity.

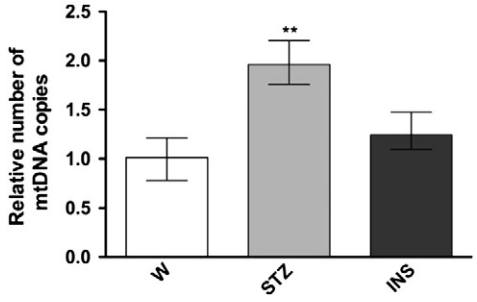

Fig. 5. Effects of T1D (STZ-induced diabetes) and insulin (INS) treatment in the number of copies of mitochondrial DNA (mtDNA). Data are the median ± interquartile range of 5 animals from each condition studied. Statistical significance: **$p < 0.01$ when compared to the respective Wistar (W) control animals.

4. Discussion

T1D patients critically depend on lifelong INS treatment to survive. Indeed, T1D leads to several long-term complications due to the extremely high levels of blood glucose, which is expected to be controlled by INS therapy [28–30].

STZ administration significantly increased glycemia and HbA1c levels and avoided body weight gain (Table 2). The daily s.c. administration of INS ameliorated the levels of blood glucose and HbA1c. Strikingly, INS treatment also induced a significant body weight gain when compared to diabetic animals (Table 2). The phenotypic effects induced by STZ injection are comparable to those described by others in STZ-induced diabetic animals [18,31,32] and T1D patients [33]. Nevertheless, the levels of glucose (Fig. 1B) and pyruvate (Fig. 1C) in cerebral cortex of diabetic rats remained statistically unchanged suggesting that glucose uptake and its metabolism by glycolysis are unaffected in this animal model of T1D. It was previously reported that the function of glucose transporter 1 (GLUT 1), the main glucose transporter found in the blood–brain barrier (BBB), is not altered in cerebral microvessels of diabetic rats [34]. In addition, an increase in glucose use was reported throughout the brain 1 week after STZ administration in rats, while normal rates were found 4 weeks after diabetes induction [35]. The systemic characterization of the INS-treated animals (Table 2) and the levels of INS found in the brains of these animals (Fig. 1A) show the effectiveness of the INS treatment. The increase in glucose levels in INS-treated diabetic rats is not related with alterations in glucose utilization since the levels of pyruvate (Fig. 1C) and mitochondrial function (Table 3) remained statistically unaltered. The increase in glucose levels in INS-

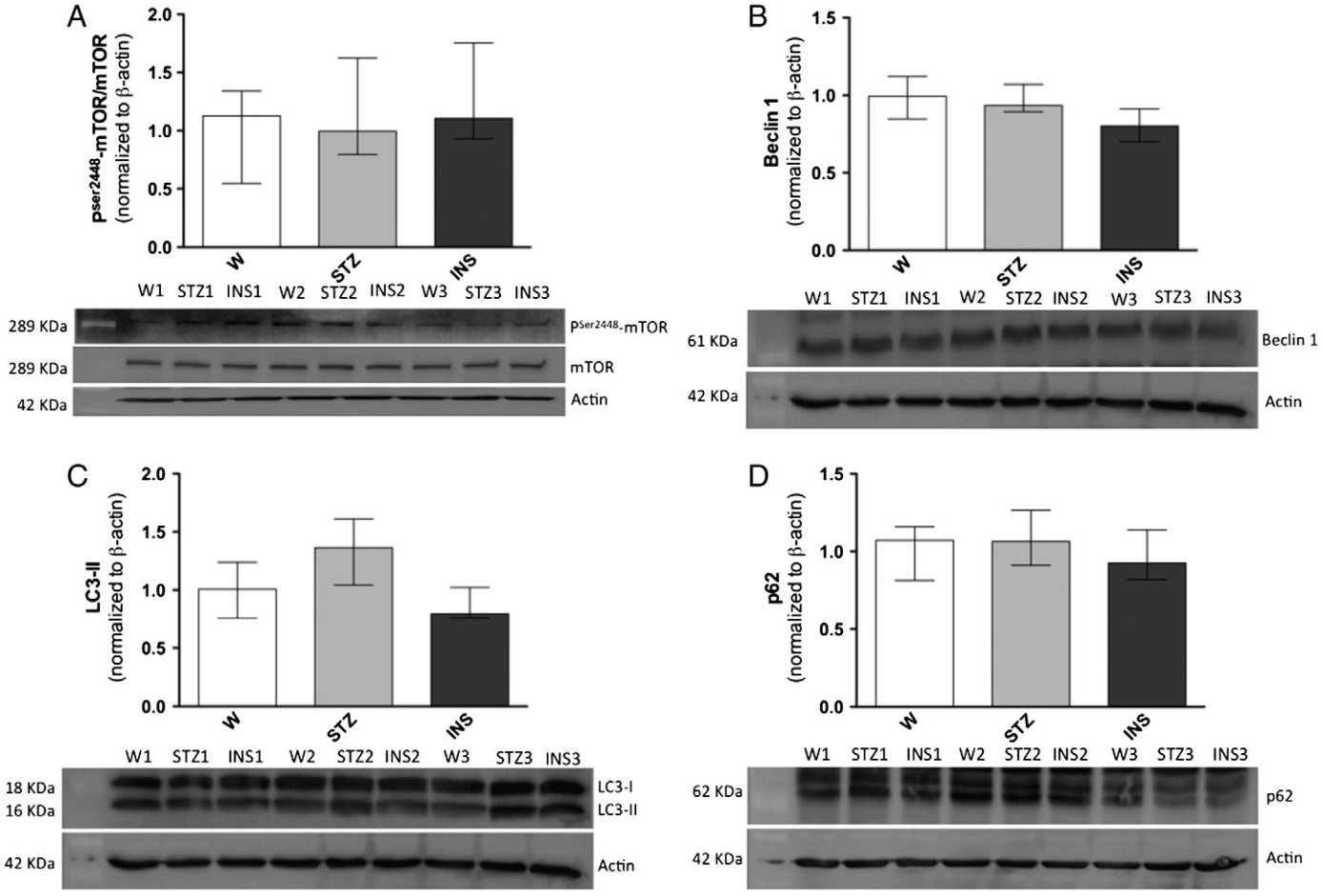

Fig. 6. Effects of T1D (STZ-induced diabetes) and insulin (INS) treatment in the levels of autophagy-related proteins: $P^{ser2448}$-mTOR/mTOR (A), Beclin1 (B), LC3-II (C), p62 (D). Data are the median ± interquartile range of 6 animals from each condition studied.

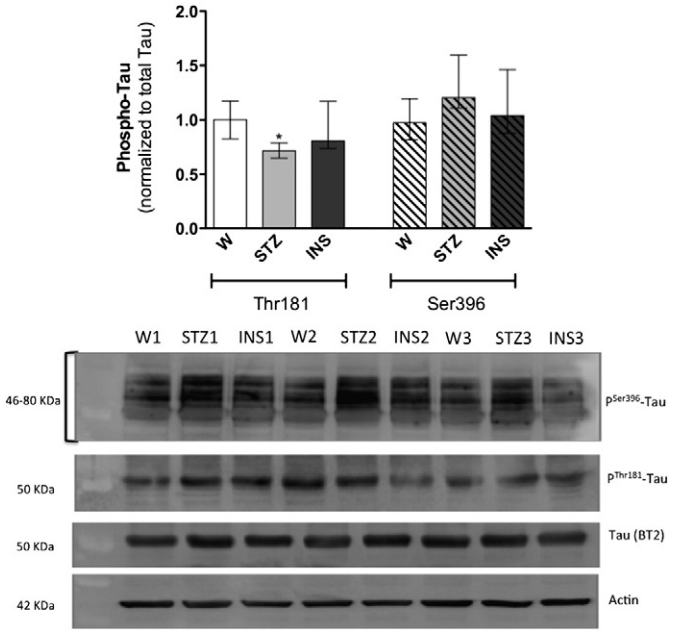

Fig. 7. Effects of T1D (STZ-induced diabetes) and insulin (INS) treatment on the ratio between phosphorylated (Thr181 and Ser396 residues) tau and total tau protein levels. Data are the median ± interquartile range of 6 animals from each condition studied. Statistical significance: *$p < 0.05$ when compared to the respective Wistar (W) control animals.

treated diabetic brains may represent a stimulatory action of INS in promoting glucose uptake into the brain.

INS treatment partially reversed the increase in the ratio of tau phosphorylated at Ser396 to total tau promoted by STZ-induced diabetes (Fig. 7). Our results converge with other studies showing an increased phosphorylation of tau protein in the brains of STZ diabetic animals [36,37]. In vitro, pseudophosphorylation of Ser396 and Ser404 generates tau that is more fibrillogenic [38]. Mutational studies with human tau also showed that phosphorylation of tau at Ser396 is primarily responsible for the functional loss of tau-mediated tubulin polymerization [39]. Interestingly, the ratio of tau phosphorylated at Thr181 to total tau is decreased in the brain cortices of STZ diabetic animals (Fig. 7). A protective role for tau phosphorylation could be suggested when that modification take place at Thr181 [40], which could facilitate its binding to exosomes and the release of tau excess [41]. Under these circumstances, the decrease in the ratio of tau phosphorylated at Thr181 to total tau observed in the brains of STZ-induced diabetic rats may indicate an increased probability for an over accumulation and deposition of tau.

Several mechanisms modulate tau protein phosphorylation levels, such as the decrease in the activity of PP2A, as observed in the brains of STZ animals and spontaneous model of T1D, the non-obese diabetic (NOD) mouse [36,37,42]. Accordingly, we observed a non-statistically significant decrease of PP2A activity in the cerebral cortex of STZ diabetic rats (Fig. 9). It was also reported that the active form of p38-MAPK was increased in neurons from the olfactory bulb of STZ diabetic rats, which was accompanied by an increase in tau protein phosphorylation [43]. Moreover, Clodfelder-Miller et al. [44] reported that STZ diabetic animals present an increase in p38 MAPK and JNK active forms while

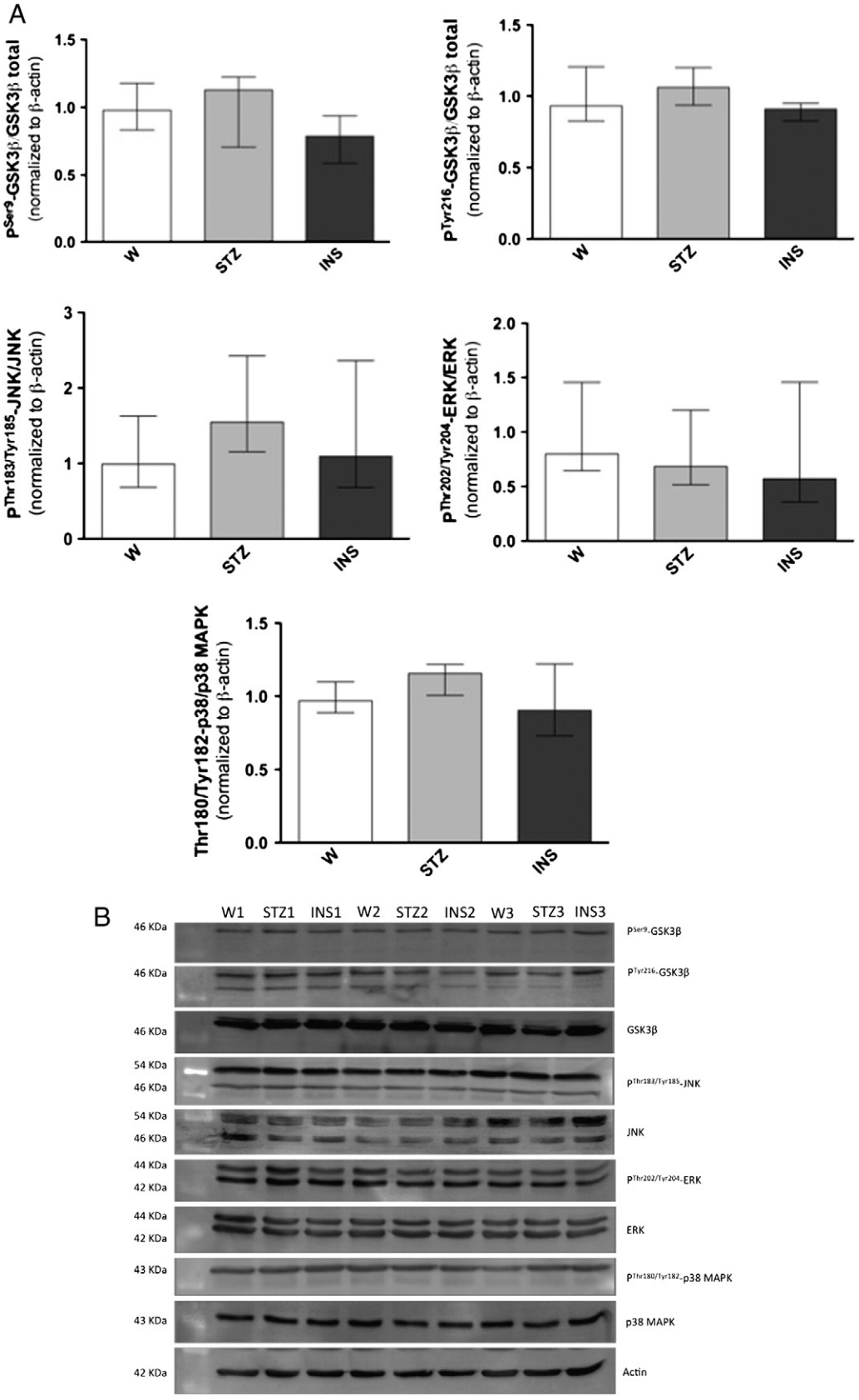

Fig. 8. Effects of T1D (STZ-induced diabetes) and insulin (INS) treatment in the phosphorylation of several kinases: GSK3β, JNK, ERK and p38 MAPK (A and B). Data are the median ± interquartile range of 6 animals from each condition studied.

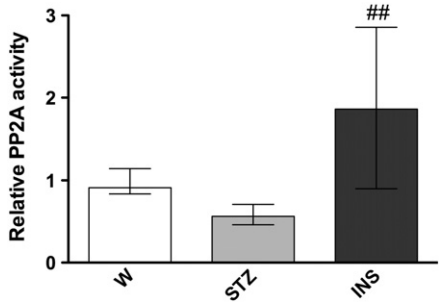

Fig. 9. Effects of T1D (STZ-induced diabetes) and insulin (INS) treatment in the activity of protein phosphatase 2A (PP2A). Data are the median ± interquartile range of 6 animals from each condition studied. Statistical significance: $^{\#\#}p < 0.01$ when compared to the respective STZ diabetic animals.

ERK remains unchanged. However, in our study, no significant alterations were observed in the active forms of p38-MAPK and JNK (Fig. 8A and B).

The decrease in the levels of phosphorylated tau protein promoted by INS treatment can be explained, at least in part, by the slight decrease in the levels of the active form of the Ser/Thr kinase GSK3β (P^{Tyr216}-GSK3β) (Fig. 8A and B). Duarte et al. [45] showed that insulin decreased P^{Tyr216}-GSK3β phosphorylation in vitro. Additionally, INS treatment significantly increased the activity of PP2A (Fig. 9), contributing to the normalization of the levels of phosphorylated tau protein. Ho and collaborators [46] demonstrated that insulin and IGF-1 reduce tau protein phosphorylation via the PI3-K pathway promoting its binding to microtubules. It was also shown that intranasal administration of insulin ameliorated tau protein phosphorylation in type 2 diabetic mice [47].

Also, the slight decrease in LC3-II levels observed in INS-treated animals (Fig. 6C), which suggest a decrease in autophagy, can be correlated with the decrease in tau protein phosphorylation via stimulation of tau proteolysis by activation of calpains [48]. Indeed, Zhang et al. [48] demonstrated that inhibition of autophagy with 3-methyladenine (3-MA) elicited an increased calpain activity and, concomitantly, a reduction in the levels of phosphorylated tau protein. The decrease in LC3-II levels in INS-treated animals may result from the stimulation of mTOR activity by INS [49]. However, unexpectedly, the levels of both $P^{ser2448}$-mTOR (Fig. 6A), an active form of the autophagy repressor, and Beclin1 (Fig. 6B), an autophagy inducer, remained unaltered. Nonetheless, it is noteworthy that mTOR phosphorylation does not always correlate with its activity [50]. It has been also reported that the activation of mTOR may occur when one of the three residues (T2446, S2448 and S2481) is phosphorylated [51]. Additionally, p62, an autophagic substrate, also remained unchanged in both experimental groups when compared to the control group (Fig. 6 D). This result regarding the levels of p62 is quite surprising taking into account the levels of LC3-II (Fig. 6). Indeed, it is expectable that when autophagy is inhibited, as suggested by the decrease in LC3-II in INS-treated animals (Fig. 6 C), the levels of p62 increase [52]. However, p62 is also involved in proteasomal degradation [53], which indicate that the relation between autophagy and p62 levels is not always straightforward.

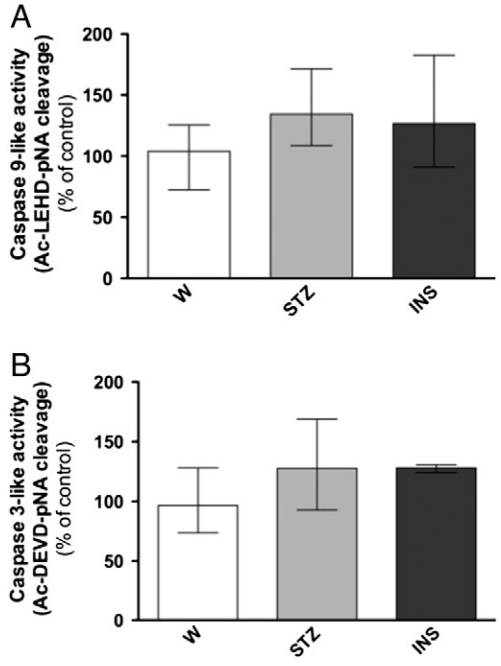

Fig 10. Effects of T1D (STZ-induced diabetes) and insulin (INS) treatment in the caspase 9- (A) and caspase 3-like (B) activities. Data are the median ± interquartile range of 5 animals from each condition studied.

It has been described that tau protein hyperphosphorylation causes mitochondrial dynamics abnormalities such as changes in mitochondrial distribution [54], and mitochondrial enlargement [55], which is putatively due to an abnormal interaction between the mitochondrial fission protein DRP1 and hyperphosphorylated tau protein [56]. In our model of T1D, the expression pattern of the proteins involved in mitochondrial fusion and fission is more compatible with enhanced mitochondrial fragmentation due to increased phosphorylation of DRP1 at Ser616 (Fig. 3B). In agreement with our observations, increased mitochondrial fission associated to increased protein levels of Fis1 and DRP1 was observed in venous endothelial cells from patients with diabetes [57]. INS treatment reversed the increase in P^{ser616}-DRP1 (Fig. 3B) promoted by STZ-induced T1D. Also the observation that OPA1 protein levels remained unaltered (Fig. 2C) in both STZ- and INS-treated animals is consistent with the unaltered activity of caspases 9 and 3 (Fig. 10). Only 10–15% of cytochrome c is found free in the intermembrane space, while the major fraction can be found in the cristae [58,59]. OPA1 complexes are involved in cristae remodeling, and the assembly and disassembly of such complexes regulates cytochrome c release from inside the cristae, and therefore caspase-dependent apoptotic cell death [60,61].

There is scarce evidence about the role of hyperglycemia in mitochondrial biogenesis, particularly in the central nervous system. A nuclear-mitochondrial crosstalk regulates mitochondria biogenesis via PGC1α-NRF1/2-TFAM [61,62]. Indeed, Edwards et al. [63] demonstrated in a mouse model of type 2 diabetes (T2D) with well-established diabetic neuropathy, that neurons from the dorsal root ganglia (DRG) presented greater mitochondrial biogenesis, when compared with non-diabetic mice. Also in vitro experiments demonstrated that cultured DRG exposed to hyperglycemic conditions exhibited increased mitochondrial biogenesis [63,64]. The authors proposed that the increase in mitochondrial biogenesis is occurring in an attempt to overcome the metabolic load induced by the hyperglycemic status as well as to compensate for the enhanced mitochondrial fragmentation [63,64]. Accordingly, we also observed an increase in mitochondrial biogenesis through the increase in the levels of NRF2 (Fig. 4B) and TFAM levels (Fig. 4C) and mtDNA copy number (Fig. 5) in T1D animals, those effects being normalized by INS treatment. Studies performed in primary cultures of mice hepatocytes revealed that prolonged exposure to INS decreased the levels of NRF1, TFAM and the cellular mitochondrial content [65]. The alterations in mitochondrial biogenesis occurring in the cerebral cortex of T1D animals may represent a compensation mechanism against mitochondrial fragmentation, since there is no alteration of mitochondrial function (Table 3) and no activation of the apoptotic cascade (Fig. 10A and B), which protect synapse integrity, as demonstrated by the maintenance of synaptophysin and PSD95 levels (Fig. 11), two proteins crucial for neurotransmission and synaptic plasticity [66]. Accordingly, it has been recently demonstrated by our group, that

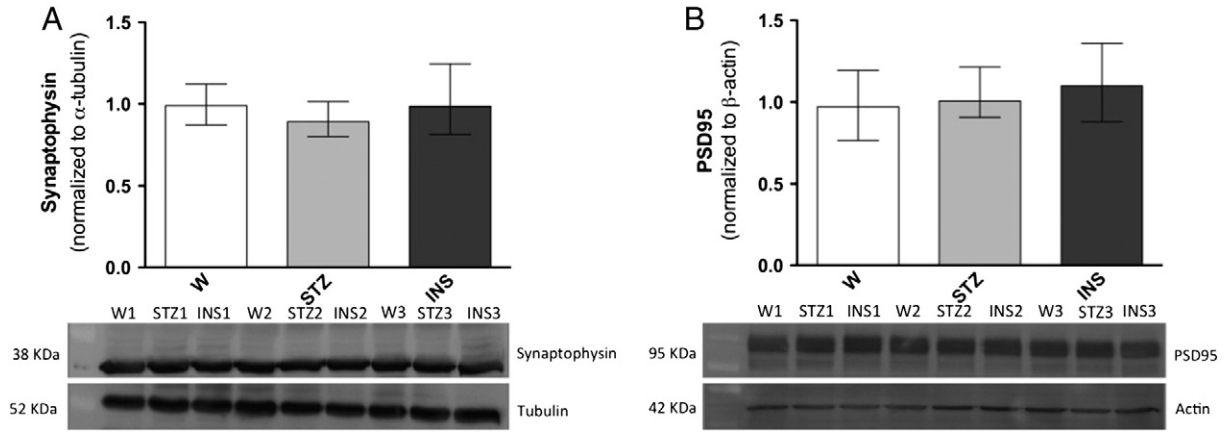

Fig. 11. Effects of T1D (STZ-induced diabetes) and insulin (INS) treatment in the protein levels of synaptophysin (A) and PSD95 (B). Data are the median ± interquartile range of 6 animals from each condition studied.

mitochondria isolated from the cortex of T1D animals did not show significant alterations neither in the respiratory chain nor in the phosphorylation system [32].

5. Conclusions

Altogether our results support the idea that T1D modulates brain cortical mitochondria through possible compensatory mechanisms avoiding the decline of mitochondrial function, which is crucial for brain cells integrity and survival. Nevertheless, STZ-induced diabetes increases the abnormal phosphorylation of tau protein that in short- or medium-term may predispose to neurodegenerative events. Our study also shows beneficial effects of INS therapy that is able to normalize or attenuate brain cortical alterations promoted by STZ-induced T1D. However, longer-term studies must be done to elucidate the impact of T1D in brain biochemistry, structure and function. It would be also interesting to study the effectiveness of INS therapy after a longer period of time.

Acknowledgements

Renato X. Santos has a PhD fellowship from the Fundação para a Ciência e a Tecnologia (SFRH/BD/43972/2008). The authors' work is supported by PEst-C/SAU/LA0001/2013–2014.

References

[1] M.J. Gan, A. Albanese-O'Neill, M.J. Haller, Type 1 diabetes: current concepts in epidemiology, pathophysiology, clinical care, and research, Curr. Probl. Pediatr. Adolesc. Health Care 42 (2012) 269–291.
[2] G.J. Biessels, I.J. Deary, C.M. Ryan, Cognition and diabetes: a lifespan perspective, Lancet Neurol. 7 (2008) 184–190.
[3] C. Ryan, A. Vega, A. Drash, Cognitive deficits in adolescents who developed diabetes early in life, Pediatrics 75 (1985) 921–927.
[4] C.G. Jolivalt, R. Hurford, C.A. Lee, W. Dumaop, E. Rockenstein, E. Masliah, Type 1 diabetes exaggerates features of Alzheimer's disease in APP transgenic mice, Exp. Neurol. 223 (2010) 422–431.
[5] S. Cardoso, S. Correia, R.X. Santos, C. Carvalho, M.S. Santos, C.R. Oliveira, G. Perry, M.A. Smith, X. Zhu, P.I. Moreira, Insulin is a two-edged knife on the brain, J. Alzheimers Dis. 18 (2009) 483–507.
[6] W.Q. Zhao, H. Chen, M.J. Quon, D.L. Alkon, Insulin and the insulin receptor in experimental models of learning and memory, Eur. J. Pharmacol. 490 (2004) 71–81.
[7] S. Dore, S. Kar, R. Quirion, Insulin-like growth factor I protects and rescues hippocampal neurons against beta-amyloid- and human amylin-induced toxicity, Proc. Natl. Acad. Sci. U. S. A. 94 (1997) 4772–4777.
[8] T. Takadera, N. Sakura, T. Mohri, T. Hashimoto, Toxic effect of a beta-amyloid peptide (beta 22–35) on the hippocampal neuron and its prevention, Neurosci. Lett. 161 (1993) 41–44.
[9] M. Hong, V.M. Lee, Insulin and insulin-like growth factor-1 regulate tau phosphorylation in cultured human neurons, J. Biol. Chem. 272 (1997) 19547–19553.
[10] B. Chance, H. Sies, A. Boveris, Hydroperoxide metabolism in mammalian organs, Physiol. Rev. 59 (1979) 527–605.
[11] P.I. Moreira, X. Zhu, X. Wang, H.G. Lee, A. Nunomura, R.B. Petersen, G. Perry, M.A. Smith, Mitochondria: a therapeutic target in neurodegeneration, Biochim. Biophys. Acta 1802 (2010) 212–220.
[12] R.X. Santos, S.C. Correia, X. Wang, G. Perry, M.A. Smith, P.I. Moreira, X. Zhu, Alzheimer's disease: diverse aspects of mitochondrial malfunctioning, Int. J. Clin. Exp. Pathol. 3 (2010) 570–581.
[13] S.C. Correia, R.X. Santos, S. Cardoso, C. Carvalho, E. Candeias, A.I. Duarte, A.I. Placido, M.S. Santos, P.I. Moreira, Alzheimer disease as a vascular disorder: where do mitochondria fit? Exp. Gerontol. 47 (2012) 878–886.
[14] J.V. Virbasius, R.C. Scarpulla, Activation of the human mitochondrial transcription factor A gene by nuclear respiratory factors: a potential regulatory link between nuclear and mitochondrial gene expression in organelle biogenesis, Proc. Natl. Acad. Sci. U. S. A. 91 (1994) 1309–1313.
[15] Z. Wu, P. Puigserver, U. Andersson, C. Zhang, G. Adelmant, V. Mootha, A. Troy, S. Cinti, B. Lowell, R.C. Scarpulla, B.M. Spiegelman, Mechanisms controlling mitochondrial biogenesis and respiration through the thermogenic coactivator PGC-1, Cell 98 (1999) 115–124.
[16] R.X. Santos, S. Cardoso, S. Correia, C. Carvalho, M.S. Santos, P.I. Moreira, Targeting autophagy in the brain: a promising approach? Cent. Nerv. Syst. Agents Med. Chem. 10 (2010) 158–168.
[17] P.I. Moreira, R.X. Santos, X. Zhu, H.G. Lee, M.A. Smith, G. Casadesus, G. Perry, Autophagy in Alzheimer's disease, Expert. Rev. Neurother. 10 (2010) 1209–1218.
[18] P.I. Moreira, M.S. Santos, C. Sena, R. Seica, C.R. Oliveira, Insulin protects against amyloid beta-peptide toxicity in brain mitochondria of diabetic rats, Neurobiol. Dis. 18 (2005) 628–637.
[19] P.I. Moreira, M.S. Santos, A. Moreno, C. Oliveira, Amyloid beta-peptide promotes permeability transition pore in brain mitochondria, Biosci. Rep. 21 (2001) 789–800.
[20] A.G. Gornall, C.J. Bardawill, M.M. David, Determination of serum proteins by means of the biuret reaction, J. Biol. Chem. 177 (1949) 751–766.
[21] R.E. Estabrook, Mitochondrial respiratory control and the polarographic measurement of ADP/O ratios, Methods Enzymol. 10 (1967) 41–47.
[22] B. Chance, G.R. Williams, The respiratory chain and oxidative phosphorylation, Adv. Enzymol. Relat. Subj. Biochem. 17 (1956) 65–134.
[23] A.M. Silva, P.J. Oliveira, Evaluation of respiration with clark type electrode in isolated mitochondria and permeabilized animal cells, Methods Mol. Biol. 810 (2012) 7–24.
[24] N. Kamo, M. Muratsugu, R. Hongoh, Y. Kobatake, Membrane potential of mitochondria measured with an electrode sensitive to tetraphenyl phosphonium and relationship between proton electrochemical potential and phosphorylation potential in steady state, J. Membr. Biol. 49 (1979) 105–121.
[25] B.D. Jensen, T.R. Gunter, The use of tertaphenylphosphonium (TPP^+) to measure membrane potentials in mitochondria: membrane binding and respiratory effects, Biophys. J. 45 (1984) 92.
[26] M. Muratsugu, N. Kamo, K. Kurihara, Y. Kobatake, Selective electrode for dibenzyl dimethyl ammonium cation as indicator of the membrane potential in biological systems, Biochim. Biophys. Acta 464 (1977) 613–619.
[27] S. Fuke, M. Kubota-Sakashita, T. Kasahara, Y. Shigeyoshi, T. Kato, Regional variation in mitochondrial DNA copy number in mouse brain, Biochim. Biophys. Acta 1807 (2011) 270–274.
[28] V. Brussee, F.A. Cunningham, D.W. Zochodne, Direct insulin signaling of neurons reverses diabetic neuropathy, Diabetes 53 (2004) 1824–1830.
[29] G. Francis, J. Martinez, W. Liu, T. Nguyen, A. Ayer, J. Fine, D. Zochodne, L.R. Hanson, W.H. Frey II, C. Toth, Intranasal insulin ameliorates experimental diabetic neuropathy, Diabetes 58 (2009) 934–945.
[30] P. Reichard, B.Y. Nilsson, U. Rosenqvist, The effect of long-term intensified insulin treatment on the development of microvascular complications of diabetes mellitus, N. Engl. J. Med. 329 (1993) 304–309.
[31] S. Cardoso, M.S. Santos, R. Seica, P.I. Moreira, Cortical and hippocampal mitochondria bioenergetics and oxidative status during hyperglycemia and/or insulin-induced hypoglycemia, Biochim. Biophys. Acta 1802 (2010) 942–951.

[32] S. Cardoso, R.X. Santos, S.C. Correia, C. Carvalho, M.S. Santos, I. Baldeiras, C.R. Oliveira, P.I. Moreira, Insulin-induced recurrent hypoglycemia exacerbates diabetic brain mitochondrial dysfunction and oxidative imbalance, Neurobiol. Dis. 49C (2012) 1–12.
[33] D.W. Cooke, L. Plotnick, Type 1 diabetes mellitus in pediatrics, Pediatr. Rev. 29 (2008) 374–384 (quiz 385).
[34] K. Shah, S. Desilva, T. Abbruscato, The role of glucose transporters in brain disease: diabetes and Alzheimer's disease, Int. J. Mol. Sci. 13 (2012) 12629–12655.
[35] A.M. Mans, M.R. DeJoseph, D.W. Davis, R.A. Hawkins, Brain energy metabolism in streptozotocin-diabetes, Biochem. J. 249 (1988) 57–62.
[36] E. Planel, Y. Tatebayashi, T. Miyasaka, L. Liu, L. Wang, M. Herman, W.H. Yu, J.A. Luchsinger, B. Wadzinski, K.E. Duff, A. Takashima, Insulin dysfunction induces in vivo tau hyperphosphorylation through distinct mechanisms, J. Neurosci. 27 (2007) 13635–13648.
[37] Z. Qu, Z. Jiao, X. Sun, Y. Zhao, J. Ren, G. Xu, Effects of streptozotocin-induced diabetes on tau phosphorylation in the rat brain, Brain Res. 1383 (2011) 300–306.
[38] A. Abraha, N. Ghoshal, T.C. Gamblin, V. Cryns, R.W. Berry, J. Kuret, L.I. Binder, C-terminal inhibition of tau assembly in vitro and in Alzheimer's disease, J. Cell Sci. 113 (2000) 3737–3745.
[39] D.B. Evans, K.B. Rank, K. Bhattacharya, D.R. Thomsen, M.E. Gurney, S.K. Sharma, Tau phosphorylation at serine 396 and serine 404 by human recombinant tau protein kinase II inhibits tau's ability to promote microtubule assembly, J. Biol. Chem. 275 (2000) 24977–24983.
[40] D. Simón, E. García-García, F. Royo, J.M. Falcón-Pérez, J. Avila, Proteostasis of tau. Tau overexpression results in its secretion via membrane vesicles, FEBS Lett. 586 (2012) 47–54.
[41] G.V. Johnson, R.S. Jope, L.I. Binder, Proteolysis of tau by calpain, Biochem. Biophys. Res. Commun. 163 (1989) 1505–1511.
[42] M.A. Papon, N.B. El Khoury, F. Marcouiller, C. Julien, F. Morin, A. Bretteville, F.R. Petry, S. Gaudreau, A. Amrani, P.M. Mathews, S.S. Hebert, E. Planel, Deregulation of protein phosphatase 2A and hyperphosphorylation of tau protein following onset of diabetes in NOD mice, Diabetes 62 (2013) 609–617.
[43] R. Sharma, E. Buras, T. Terashima, F. Serrano, C.A. Massaad, L. Hu, B. Bitner, T. Inoue, L. Chan, R.G. Pautler, Hyperglycemia induces oxidative stress and impairs axonal transport rates in mice, PLoS One 5 (2010) e13463.
[44] B.J. Clodfelder-Miller, A.A. Zmijewska, G.V. Johnson, R.S. Jope, Tau is hyperphosphorylated at multiple sites in mouse brain in vivo after streptozotocin-induced insulin deficiency, Diabetes 55 (2006) 3320–3325.
[45] A.I. Duarte, P. Santos, C.R. Oliveira, M.S. Santos, A.C. Rego, Insulin neuroprotection against oxidative stress is mediated by Akt and GSK-3beta signaling pathways and changes in protein expression, Biochim. Biophys. Acta 1783 (2008) 994–1002.
[46] L. Ho, W. Qin, P.N. Pompl, Z. Xiang, J. Wang, Z. Zhao, Y. Peng, G. Cambareri, A. Rocher, C.V. Mobbs, P.R. Hof, G.M. Pasinetti, Diet-induced insulin resistance promotes amyloidosis in a transgenic mouse model of Alzheimer's disease, FASEB J. 18 (2004) 902–904.
[47] Y. Yang, J. Zhang, D. Ma, M. Zhang, S. Hu, S. Shao, C.X. Gong, Subcutaneous administration of liraglutide ameliorates Alzheimer-associated tau hyperphosphorylation in rats with type 2 diabetes, J. Alzheimers Dis. 37 (2013) 637–648.
[48] J.Y. Zhang, C. Peng, H. Shi, S. Wang, Q. Wang, J.Z. Wang, Inhibition of autophagy causes tau proteolysis by activating calpain in rat brain, J. Alzheimers Dis. 16 (2009) 39–47.
[49] P.H. Scott, G.J. Brunn, A.D. Kohn, R.A. Roth, J.C. Jr Lawrence JC, Evidence of insulin-stimulated phosphorylation and activation of the mammalian target of rapamycin mediated by a protein kinase B signaling pathway, Proc. Natl. Acad. Sci. U. S. A. 95 (1998) 7772–7777.
[50] A. Caccamo, S. Majumder, A. Richardson, R. Strong, S. Oddo, Molecular interplay between mammalian target of rapamycin (mTOR), amyloid-beta, and Tau: effects on cognitive impairments, J. Biol. Chem. 285 (2010) 13107–13120.
[51] J. Copp, G. Manning, T. Hunter, TORC-specific phosphorylation of mammalian target of rapamycin (mTOR): phospho-Ser2481 is a marker for intact mTOR signaling complex 2, Cancer Res. 69 (2009) 1821–1827.
[52] D.J. Klionsky, F.C. Abdalla, H. Abeliovich, R.T. Abraham, A. Acevedo-Arozena, K. Adeli, L. Agholme, M. Agnello, P. Agostinis, J.A. Aguirre-Ghiso, H.J. Ahn, O. Ait-Mohamed, S. Ait-Si-Ali, T. Akematsu, S. Akira, H.M. Al-Younes, M.A. Al-Zeer, M.L. Albert, R.L. Albin, J. Alegre-Abarrategui, M.F. Aleo, M. Alirezaei, A. Almasan, M. Almonte-Becerril, A. Amano, R. Amaravadi, S. Amarnath, A.O. Amer, N. Andrieu-Abadie, V. Anantharam, D.K. Ann, S. Anoopkumar-Dukie, H. Aoki, N. Apostolova, G. Arancia, J.P. Aris, K. Asanuma, N.Y. Asare, H. Ashida, V. Askanas, D.S. Askew, P. Auberger, M. Baba, S.K. Backues, E.H. Baehrecke, B.A. Bahr, X.Y. Bai, Y. Bailly, R. Baiocchi, G. Baldini, W. Balduini, A. Ballabio, B.A. Bamber, E.T. Bampton, G. Banhegyi, C.R. Bartholomew, D. C. Bassham, R.C. Bast Jr., H. Batoko, B.H. Bay, I. Beau, D.M. Bechet, T.J. Begley, C. Behl, C. Behrends, S. Bekri, B. Bellaire, L.J. Bendall, L. Benetti, L. Berliocchi, H. Bernardi, F. Bernassola, S. Besteiro, I. Bhatia-Kissova, X. Bi, M. Biard-Piechaczyk, J.S. Blum, L.H. Boise, P. Bonaldo, D.L. Boone, B.C. Bornhauser, K.R. Bortoluci, I. Bossis, F. Bost, J.P. Bourquin, P. Boya, M. Boyer-Guittaut, P.V. Bozhkov, N.R. Brady, C. Brancolini, A. Brech, J.E. Brenman, A. Brennand, E.H. Bresnick, P. Brest, D. Bridges, M.L. Bristol, P.S. Brookes, E.J. Brown, J.H. Brumell, N. Brunetti-Pierri, U.T. Brunk, D. E. Bulman, S.J. Bultman, G. Bultynck, L.F. Burbulla, W. Bursch, J.P. Butchar, W. Buzgariu, S.P. Bydlowski, K. Cadwell, M. Cahova, D. Cai, J. Cai, Q. Cai, B. Calabretta, J. Calvo-Garrido, N. Camougrand, M. Campanella, J. Campos-Salinas, E. Candi, L. Cao, A.B. Caplan, S.R. Carding, S.M. Cardoso, J.S. Carew, C.R. Carlin, V. Carmignac, L. A. Carneiro, S. Carra, R.A. Caruso, G. Casari, C. Casas, R. Castino, E. Cebollero, F. Cecconi, J. Celli, H. Chaachouay, H.J. Chae, C.Y. Chai, D.C. Chan, E.Y. Chan, R.C. Chang, C.M. Che, C.C. Chen, G.C. Chen, G.Q. Chen, M. Chen, Q. Chen, S.S. Chen, W. Chen, X. Chen, Y.G. Chen, Y. Chen, Y.J. Chen, Z. Chen, A. Cheng, C.H. Cheng, Y. Cheng, H. Cheong, J.H. Cheong, S. Cherry, R. Chess-Williams, Z.H. Cheung, E. Chevet, H.L. Chiang, R. Chiarelli, T. Chiba, L.S. Chin, S.H. Chiou, F.V. Chisari, C.H. Cho, D.H. Cho, A.M. Choi, D. Choi, K.S. Choi, M.E. Choi, S. Chouaib, D. Choubey, V. Choubey, C.T. Chu, T.H. Chuang, S.H. Chueh, T. Chun, Y.J. Chwae, M.L. Chye, R. Ciarcia, M.R. Ciriolo, M.J. Clague, R.S. Clark, P.G. Clarke, R. Clarke, P. Codogno, H.A. Coller, M.I. Colombo, S. Comincini, M. Condello, F. Condorelli, M.R. Cookson, G.H. Coombs, I. Coppens, R. Corbalan, P. Cossart, P. Costelli, S. Costes, A. Coto-Montes, E. Couve, F.P. Coxon, J.M. Cregg, J.L. Crespo, M.J. Cronje, A.M. Cuervo, J.J. Cullen, M.J. Czaja, M. D'Amelio, A. Darfeuille-Michaud, L.M. Davids, F.E. Davies, M. De Felici, J.F. de Groot, C.A. de Haan, L. De Martino, A. De Milito, V. De Tata, J. Debnath, A. Degterev, B. Dehay, L. M. Delbridge, F. Demarchi, Y.Z. Deng, J. Dengjel, P. Dent, D. Denton, V. Deretic, S.D. Desai, R.J. Devenish, M. Di Gioacchino, G. Di Paolo, C. Di Pietro, G. Diaz-Araya, I. Diaz-Laviada, M.T. Diaz-Meco, J. Diaz-Nido, I. Dikic, S.P. Dinesh-Kumar, W.X. Ding, C.W. Distelhorst, A. Diwan, M. Djavaheri-Mergny, S. Dokudovskaya, Z. Dong, F.C. Dorsey, V. Dosenko, J.J. Dowling, S. Doxsey, M. Dreux, M.E. Drew, Q. Duan, M.A. Duchosal, K. Duff, I. Dugail, M. Durbeej, M. Duszenko, C.L. Edelstein, A.L. Edinger, G. Egea, L. Eichinger, N.T. Eissa, S. Ekmekcioglu, W.S. El-Deiry, Z. Elazar, M. Elgendy, L.M. Ellerby, K.E. Eng, A.M. Engelbrecht, S. Engelender, J. Erenpreisa, R. Escalante, A. Esclatine, E.L. Eskelinen, L. Espert, V. Espina, H. Fan, J. Fan, Q.W. Fan, Z. Fan, S. Fang, Y. Fang, M. Fanto, A. Fanzani, T. Farkas, J.C. Farre, M. Faure, M. Fechheimer, C.G. Feng, J. Feng, Q. Feng, Y. Feng, L. Fesus, R. Feuer, M.E. Figueiredo-Pereira, G.M. Fimia, D.C. Fingar, S. Finkbeiner, T. Finkel, K.D. Finley, F. Fiorito, E.A. Fisher, P.B. Fisher, M. Flajolet, M.L. Florez-McClure, S. Florio, E.A. Fon, F. Fornai, F. Fortunato, R. Fotedar, D.H. Fowler, H.S. Fox, R. Franco, L.B. Frankel, M. Fransen, J.M. Fuentes, J. Fueyo, J. Fujii, K. Fujisaki, E. Fujita, M. Fukuda, R.H. Furukawa, M. Gaestel, P. Gailly, M. Gajewska, B. Galliot, V. Galy, S. Ganesh, B. Ganetzky, I.G. Ganley, F.B. Gao, G.F. Gao, J. Gao, L. Garcia, G. Garcia-Manero, M. Garcia-Marcos, M. Garmyn, A.L. Gartel, E. Gatti, M. Gautel, T.R. Gawriluk, M.E. Gegg, J. Geng, M. Germain, J.E. Gestwicki, D.A. Gewirtz, S. Ghavami, P. Ghosh, A.M. Giammarioli, A.N. Giatromanolaki, S.B. Gibson, R.W. Gilkerson, M.L. Ginger, H.N. Ginsberg, J. Golab, M.S. Goligorsky, P. Golstein, C. Gomez-Manzano, E. Goncu, C. Gongora, C.D. Gonzalez, R. Gonzalez, C. Gonzalez-Estevez, R.A. Gonzalez-Polo, E. Gonzalez-Rey, N.V. Gorbunov, S. Gorski, S. Goruppi, R.A. Gottlieb, D. Gozuacik, G.E. Granato, G.D. Grant, K.N. Green, A. Gregorc, F. Gros, C. Grose, T.W. Grunt, P. Gual, J.L. Guan, K.L. Guan, S.M. Guichard, A.S. Gukovskaya, I. Gukovsky, J. Gunst, A.B. Gustafsson, A.J. Halayko, A.N. Hale, S.K. Halonen, M. Hamasaki, F. Han, T. Han, M.K. Hancock, M. Hansen, H. Harada, M. Harada, S.E. Hardt, J.W. Harper, A.L. Harris, J. Harris, S.D. Harris, M. Hashimoto, J.A. Haspel, S. Hayashi, L.A. Hazelhurst, C. He, Y.W. He, M.J. Hebert, K.A. Heidenreich, M.H. Helfrich, G.V. Helgason, E.P. Henske, B. Herman, P.K. Herman, C. Hetz, S. Hilfiker, J.A. Hill, L.J. Hocking, P. Hofman, T.G. Hofmann, J. Hohfeld, T.L. Holyoake, M.H. Hong, D.A. Hood, G.S. Hotamisligil, E.J. Houwerzijl, M. Hoyer-Hansen, B. Hu, C.A. Hu, H.M. Hu, Y. Hua, C. Huang, J. Huang, S. Huang, W.P. Huang, T.B. Huber, W.K. Huh, T.H. Hung, T.R. Hupp, G.M. Hur, J.B. Hurley, S.N. Hussain, P.J. Hussey, J.J. Hwang, S. Hwang, A. Ichihara, S. Ilkhanizadeh, K. Inoki, T. Into, V. Iovane, J.L. Iovanna, N.Y. Ip, Y. Isaka, H. Ishida, C. Isidoro, K. Isobe, A. Iwasaki, M. Izquierdo, Y. Izumi, P.M. Jaakkola, M. Jaattela, G.R. Jackson, W.T. Jackson, B. Janji, M. Jendrach, J.H. Jeon, E.B. Jeung, H. Jiang, J.X. Jiang, M. Jiang, Q. Jiang, X. Jiang, A. Jimenez, M. Jin, S. Jin, C.O. Joe, T. Johansen, D.E. Johnson, G.V. Johnson, N.L. Jones, B. Joseph, S.K. Joseph, A.M. Joubert, G. Juhasz, L. Juillerat-Jeanneret, C.H. Jung, Y.K. Jung, K. Kaarniranta, A. Kaasik, T. Kabuta, M. Kadowaki, K. Kagedal, Y. Kamada, V.O. Kaminskyy, H.H. Kampinga, H. Kanamori, C. Kang, K.B. Kang, K.I. Kang, R. Kang, Y.A. Kang, T. Kanki, T.D. Kanneganti, H. Kanno, A.G. Kanthasamy, A. Kanthasamy, V. Karantza, G.P. Kaushal, S. Kaushik, Y. Kawazoe, P.Y. Ke, J.H. Kehrl, A. Kelekar, C. Kerkhoff, D.H. Kessel, H. Khalil, J.A. Kiel, A. A. Kiger, A. Kihara, D.R. Kim, D.H. Kim, E.K. Kim, H.R. Kim, J.S. Kim, J.H. Kim, J.C. Kim, J. K. Kim, P.K. Kim, S.W. Kim, Y.S. Kim, Y. Kim, A. Kimchi, A.C. Kimmelman, J.S. King, T.J. Kinsella, V. Kirkin, L.A. Kirshenbaum, K. Kitamoto, K. Kitazato, L. Klein, W.T. Klimecki, J. Klucken, E. Knecht, B.C. Ko, J.C. Koch, H. Koga, J.Y. Koh, Y.H. Koh, M. Koike, M. Komatsu, E. Kominami, H.J. Kong, W.J. Kong, V.I. Korolchuk, Y. Kotake, M.I. Koukourakis, J.B. Kouri Flores, A.L. Kovacs, C. Kraft, D. Krainc, H. Kramer, C. Kretz-Remy, A.M. Krichevsky, G. Kroemer, R. Kruger, O. Krut, N.T. Ktistakis, C.Y. Kuan, R. Kucharczyk, A. Kumar, R. Kumar, S. Kumar, M. Kundu, H.J. Kung, T. Kurz, H.J. Kwon, A.R. La Spada, F. Lafont, T. Lamark, J. Landry, J.D. Lane, P. Lapaquette, J.F. Laporte, L. Laszlo, S. Lavandero, J.N. Lavoie, R. Layfield, P.A. Lazo, W. Le, L. Le Cam, D.J. Ledbetter, A.J. Lee, B.W. Lee, G.M. Lee, J. Lee, J.H. Lee, M. Lee, M.S. Lee, S.H. Lee, C. Leeuwenburgh, P. Legembre, R. Legouis, M. Lehmann, H.Y. Lei, Q.Y. Lei, D.A. Leib, J. Leiro, J.J. Lemasters, A. Lemoine, M.S. Lesniak, D. Lev, V.V. Levenson, B. Levine, E. Levy, F. Li, J.L. Li, L. Li, S. Li, S. Li, W. Li, X.J. Li, Y.B. Li, Y.P. Li, C. Liang, Q. Liang, Y.F. Liao, P.P. Liberski, A. Lieberman, H.J. Lim, K.L. Lim, K. Lim, C.F. Lin, F.C. Lin, J. Lin, J.D. Lin, K. Lin, W.W. Lin, W.C. Lin, Y.L. Lin, R. Linden, P. Lingor, J. Lippincott-Schwartz, M.P. Lisanti, P.B. Liton, B. Liu, C.F. Liu, K. Liu, L. Liu, Q.A. Liu, W. Liu, Y.C. Liu, Y. Liu, R.A. Lockshin, C.N. Lok, S. Lonial, B. Loos, G. Lopez-Berestein, C. Lopez-Otin, L. Lossi, M. T. Lotze, P. Low, B. Lu, Z. Lu, F. Luciano, N.W. Lukacs, A.H. Lund, M.A. Lynch-Day, Y. Ma, F. Macian, J.P. MacKeigan, K.F. Macleod, F. Madeo, L. Maiuri, M.C. Maiuri, D. Malagoli, M.C. Malicdan, W. Malorni, N. Man, E.M. Mandelkow, S. Manon, I. Manov, K. Mao, X. Mao, Z. Mao, P. Marambaud, D. Marazziti, Y.L. Marcel, K. Marchbank, P. Marchetti, S.J. Marciniak, M. Marcondes, M. Mardi, G. Marfe, G. Marino, M. Markaki, M.R. Marten, S.J. Martin, C. Martinand-Mari, W. Martinet, M. Martinez-Vicente, M. Masini, P. Matarrese, S. Matsuo, R. Matteoni, A. Mayer, N.M. Mazure, D.J. McConkey, M.J. McConnell, C. McDermott, C. McDonald, G.M. McInerney, S.L. McKenna, B. McLaughlin, P.J. McLean, C.R. McMaster, G.A. McQuibban, A.J. Meijer, M.H. Meisler, A. Melendez, T.J. Melia, G. Melino, M.A. Mena, J.A. Menendez, R.F. Menna-Barreto, M.B. Menon, F.M. Menzies, C.A. Mercer, A. Merighi, D.E. Merry, S. Meschini, C.G. Meyer, T.F. Meyer, C.Y. Miao, J.Y. Miao, P.A. Michels, C. Michiels, D. Mijaljica, A. Milojkovic, S. Minucci, C. Miracco, C.K. Miranti, I. Mitroulis, K. Miyazawa, N. Mizushima, B. Mograbi, S. Mohseni, X. Molero, B. Mollereau, F. Mollinedo, T. Momoi, I. Monastyrska, M.M. Monick, M.J. Monteiro, M.N. Moore, R. Mora, K. Moreau, P.I. Moreira, Y. Moriyasu, J. Moscat, S. Mostowy, J.C. Mottram, T. Motyl, C.E. Moussa, S. Muller, K. Munger, C. Munz, L.O. Murphy, M.E. Murphy, A. Musaro, I.

Mysorekar, E. Nagata, K. Nagata, A. Nahimana, U. Nair, T. Nakagawa, K. Nakahira, H. Nakano, H. Nakatogawa, M. Nanjundan, N.I. Naqvi, D.P. Narendra, M. Narita, M. Navarro, S.T. Nawrocki, T.Y. Nazarko, A. Nemchenko, M.G. Netea, T.P. Neufeld, P.A. Ney, I.P. Nezis, H.P. Nguyen, D. Nie, I. Nishino, C. Nislow, R.A. Nixon, T. Noda, A.A. Noegel, A. Nogalska, S. Noguchi, L. Notterpek, I. Novak, T. Nozaki, N. Nukina, T. Nurnberger, B. Nyfeler, K. Obara, T.D. Oberley, S. Oddo, M. Ogawa, T. Ohashi, K. Okamoto, N.L. Oleinick, F.J. Oliver, L.J. Olsen, S. Olsson, O. Opota, T.F. Osborne, G.K. Ostrander, K. Otsu, J.H. Ou, M. Ouimet, M. Overholtzer, B. Ozpolat, P. Paganetti, U. Pagnini, N. Pallet, G.E. Palmer, C. Palumbo, T. Pan, T. Panaretakis, U.B. Pandey, Z. Papackova, I. Papassideri, I. Paris, J. Park, O.K. Park, J.B. Parys, K.R. Parzych, S. Patschan, C. Patterson, S. Pattingre, J.M. Pawelek, J. Peng, D.H. Perlmutter, I. Perrotta, G. Perry, S. Pervaiz, M. Peter, G.J. Peters, M. Petersen, G. Petrovski, J.M. Phang, M. Piacentini, P. Pierre, V. Pierrefite-Carle, G. Pierron, R. Pinkas-Kramarski, A. Piras, N. Piri, L.C. Platanias, S. Poggeler, M. Poirot, A. Poletti, C. Pous, M. Pozuelo-Rubio, M. Praetorius-Ibba, A. Prasad, M. Prescott, M. Priault, N. Produit-Zengaffinen, A. Progulske-Fox, T. Proikas-Cezanne, S. Przedborski, K. Przyklenk, R. Puertollano, J. Puyal, S.B. Qian, L. Qin, Z.H. Qin, S.E. Quaggin, N. Raben, H. Rabinowich, S.W. Rabkin, I. Rahman, A. Rami, G. Ramm, G. Randall, F. Randow, V.A. Rao, J.C. Rathmell, B. Ravikumar, S.K. Ray, B.H. Reed, J.C. Reed, F. Reggiori, A. Regnier-Vigouroux, A.S. Reichert, J.J. Reiners Jr., R.J. Reiter, J. Ren, J.L. Revuelta, C.J. Rhodes, K. Ritis, E. Rizzo, J. Robbins, M. Roberge, H. Roca, M.C. Roccheri, S. Rocchi, H.P. Rodemann, S. Rodriguez de Cordoba, B. Rohrer, I.B. Roninson, K. Rosen, M.M. Rost-Roszkowska, M. Rouis, K.M. Rouschop, F. Rovetta, B.P. Rubin, D.C. Rubinsztein, K. Ruckdeschel, E.B. Rucker III, A. Rudich, E. Rudolf, N. Ruiz-Opazo, R. Russo, T.E. Rusten, K.M. Ryan, S.W. Ryter, D.M. Sabatini, J. Sadoshima, T. Saha, T. Saitoh, H. Sakagami, Y. Sakai, G. H. Salekdeh, P. Salomoni, P.M. Salvaterra, G. Salvesen, R. Salvioli, A.M. Sanchez, J.A. Sanchez-Alcazar, R. Sanchez-Prieto, M. Sandri, U. Sankar, P. Sansanwal, L. Santambrogio, S. Saran, S. Sarkar, M. Sarwal, C. Sasakawa, A. Sasnauskiene, M. Sass, K. Sato, M. Sato, A.H. Schapira, M. Scharl, H.M. Schatzl, W. Scheper, S. Schiaffino, C. Schneider, M.E. Schneider, R. Schneider-Stock, P.V. Schoenlein, D.F. Schorderet, C. Schuller, G.K. Schwartz, L. Scorrano, L. Sealy, P.O. Seglen, J. Segura-Aguilar, I. Seiliez, O. Seleverstov, C. Sell, J.B. Seo, D. Separovic, V. Setaluri, T. Setoguchi, C. Settembre, J.J. Shacka, M. Shanmugam, I.M. Shapiro, E. Shaulian, R.J. Shaw, J.H. Shelhamer, H.M. Shen, W.C. Shen, Z.H. Sheng, Y. Shi, K. Shibuya, Y. Shidoji, J.J. Shieh, C.M. Shih, Y. Shimada, S. Shimizu, T. Shintani, O.S. Shirihai, G.C. Shore, A.A. Sibirny, S.B. Sidhu, B. Sikorska, E.C. Silva-Zacarin, A. Simmons, A.K. Simon, H.U. Simon, C. Simone, A. Simonsen, D.A. Sinclair, R. Singh, D. Sinha, F.A. Sinicrope, A. Sirko, P.M. Siu, E. Sivridis, V. Skop, V.P. Skulachev, R.S. Slack, S.S. Smaili, D.R. Smith, M.S. Soengas, T. Soldati, X. Song, A.K. Sood, T.W. Soong, F. Sotgia, S.A. Spector, C.D. Spies, W. Springer, S.M. Srinivasula, L. Stefanis, J.S. Steffan, R. Stendel, H. Stenmark, A. Stephanou, S.T. Stern, C. Sternberg, B. Stork, P. Stralfors, C.S. Subauste, X. Sui, D. Sulzer, J. Sun, S.Y. Sun, Z.J. Sun, J.J. Sung, K. Suzuki, T. Suzuki, M.S. Swanson, C. Swanton, S.T. Sweeney, L.K. Sy, G. Szabadkai, I. Tabas, H. Taegtmeyer, M. Tafani, K. Takacs-Vellai, Y. Takano, K. Takegawa, G. Takemura, F. Takeshita, N.J. Talbot, K.S. Tan, K. Tanaka, D. Tang, I. Tanida, B.A. Tannous, N. Tavernarakis, G.S. Taylor, G.A. Taylor, J.P. Taylor, L.S. Terada, A. Terman, G. Tettamanti, K. Thevissen, C.B. Thompson, A. Thorburn, M. Thumm, F. Tian, Y. Tian, G. Tocchini-Valentini, A.M. Tolkovsky, Y. Tomino, L. Tonges, S.A. Tooze, C. Tournier, J. Tower, R. Towns, V. Trajkovic, L.H. Travassos, T.F. Tsai, M.P. Tschan, T. Tsubata, A. Tsung, B. Turk, L.S. Turner, S.C. Tyagi, Y. Uchiyama, T. Ueno, M. Umekawa, R. Umemiya-Shirafuji, V.K. Unni, M.I. Vaccaro, E.M. Valente, G. Van den Berghe, I.J. van der Klei, W. van Doorn, L.F. van Dyk, M. van Egmond, L.A. van Grunsven, P. Vandenabeele, W.P. Vandenberghe, I. Vanhorebeek, E.C. Vaquero, G. Velasco, T. Vellai, J.M. Vicencio, R.D. Vierstra, M. Vila, C. Vindis, G. Viola, M.T. Viscomi, O.V. Voitsekhovskaja, C. von Haefen, M. Votruba, K. Wada, R. Wade-Martins, C.L. Walker, C.M. Walsh, J. Walter, X.B. Wan, A. Wang, C. Wang, D. Wang, F. Wang, G. Wang, H. Wang, H.G. Wang, H.D. Wang, J. Wang, K. Wang, M. Wang, R.C. Wang, X. Wang, Y.J. Wang, Y. Wang, Z. Wang, Z.C. Wang, D.G. Wansink, D.M. Ward, H. Watada, S.L. Waters, P. Webster, L. Wei, C.C. Weihl, W.A. Weiss, S.M. Welford, L.P. Wen, C.A. Whitehouse, J.L. Whitton, A.J. Whitworth, T. Wileman, J.W. Wiley, S. Wilkinson, D. Willbold, R.L. Williams, P.R. Williamson, B.G. Wouters, C. Wu, D.C. Wu, W. K. Wu, A. Wyttenbach, R.J. Xavier, Z. Xi, P. Xia, G. Xiao, Z. Xie, D.Z. Xu, J. Xu, L. Xu, X. Xu, A. Yamamoto, S. Yamashina, M. Yamashita, X. Yan, M. Yanagida, D.S. Yang, E. Yang, J.M. Yang, S.Y. Yang, W. Yang, W.Y. Yang, Z. Yang, M.C. Yao, T.P. Yao, B. Yeganeh, W.L. Yen, J.J. Yin, X.M. Yin, O.J. Yoo, G. Yoon, S.Y. Yoon, T. Yorimitsu, Y. Yoshikawa, T. Yoshimori, K. Yoshimoto, H.J. You, R.J. Youle, A. Younes, L. Yu, S.W. Yu, W.H. Yu, Z.M. Yuan, Z. Yue, C.H. Yun, M. Yuzaki, O. Zabirnyk, E. Silva-Zacarin, D. Zacks, E. Zacksenhaus, N. Zaffaroni, Z. Zakeri, H.J. Zeh III, S.O. Zeitlin, H. Zhang, H.L. Zhang, J. Zhang, J.P. Zhang, L. Zhang, M.Y. Zhang, X.D. Zhang, M. Zhao, Y.F. Zhao, Y. Zhao, Z.J. Zhao, X. Zheng, B. Zhivotovsky, Q. Zhong, C.Z. Zhou, C. Zhu, W.G. Zhu, X.F. Zhu, X. Zhu, Y. Zhu, T. Zoladek, W.X. Zong, A. Zorzano, J. Zschocke, B. Zuckerbraun, Guidelines for the use and interpretation of assays for monitoring autophagy, Autophagy 8 (2012) 445–544.

[53] M.L. Seibenhener, J.R. Babu, T. Geetha, H.C. Wong, N.R. Krishna, M.W. Wooten, Sequestosome 1/p62 is a polyubiquitin chain binding protein involved in ubiquitin proteasome degradation, Mol. Cell. Biol. 24 (2004) 8055–8068.

[54] K.J. Kopeikina, G.A. Carlson, R. Pitstick, A.E. Ludvigson, A. Peters, J.I. Luebke, R.M. Koffie, M.P. Frosch, B.T. Hyman, T.L. Spires-Jones, Tau accumulation causes mitochondrial distribution deficits in neurons in a mouse model of tauopathy and in human Alzheimer's disease brain, Am. J. Pathol. 179 (2011) 2071–2082.

[55] B. DuBoff, J. Gotz, M.B. Feany, Tau promotes neurodegeneration via DRP1 mislocalization in vivo, Neuron 75 (2012) 618–632.

[56] M. Manczak, P.H. Reddy, Abnormal interaction between the mitochondrial fission protein Drp1 and hyperphosphorylated tau in Alzheimer's disease neurons: implications for mitochondrial dysfunction and neuronal damage, Hum. Mol. Genet. 21 (2012) 2538–2547.

[57] S.M. Shenouda, M.E. Widlansky, K. Chen, G. Xu, M. Holbrook, C.E. Tabit, N.M. Hamburg, A.A. Frame, T.L. Caiano, M.A. Kluge, M.A. Duess, A. Levit, B. Kim, M.L. Hartman, L. Joseph, O.S. Shirihai, J.A. Vita, Altered mitochondrial dynamics contributes to endothelial dysfunction in diabetes mellitus, Circulation 124 (2011) 444–453.

[58] P. Bernardi, G.F. Azzone, Cytochrome c as an electron shuttle between the outer and inner mitochondrial membranes, J. Biol. Chem. 256 (1981) 7187–7192.

[59] L. Scorrano, M. Ashiya, K. Buttle, S. Weiler, S.A. Oakes, C.A. Mannella, S.J. Korsmeyer, A distinct pathway remodels mitochondrial cristae and mobilizes cytochrome c during apoptosis, Dev. Cell 2 (2002) 55–67.

[60] R. Yamaguchi, G. Perkins, Dynamics of mitochondrial structure during apoptosis and the enigma of Opa1, Biochim. Biophys. Acta 1787 (2009) 963–972.

[61] R.C. Scarpulla, Nuclear control of respiratory gene expression in mammalian cells, J. Cell. Biochem. 97 (2006) 673–683.

[62] R.C. Scarpulla, Transcriptional paradigms in mammalian mitochondrial biogenesis and function, Physiol. Rev. 88 (2008) 611–638.

[63] J.L. Edwards, A. Quattrini, S.I. Lentz, C. Figueroa-Romero, F. Cerri, C. Backus, Y. Hong, E.L. Feldman, Diabetes regulates mitochondrial biogenesis and fission in mouse neurons, Diabetologia 53 (2010) 160–169.

[64] A.M. Vincent, J.L. Edwards, L.L. McLean, Y. Hong, F. Cerri, I. Lopez, A. Quattrini, E.L. Feldman, Mitochondrial biogenesis and fission in axons in cell culture and animal models of diabetic neuropathy, Acta Neuropathol. 120 (2010) 477–489.

[65] H.Y. Liu, E. Yehuda-Shnaidman, T. Hong, J. Han, J. Pi, Z. Liu, W. Cao, Prolonged exposure to insulin suppresses mitochondrial production in primary hepatocytes, J. Biol. Chem. 284 (2009) 14087–14095.

[66] F. Valtorta, M. Pennuto, D. Bonanomi, F. Benfenati, Synaptophysin: leading actor or walk-on role in synaptic vesicle exocytosis? Bioessays 26 (2004) 445–453